A Novel Bioelastomer Platform with Tailorable Design Parameters for Cartilage Regeneration

by

Yue Qin

A dissertation submitted in partial fulfillment
of the requirements for the degree of
Doctor of Philosophy
(Biomedical Engineering)
in the University of Michigan
2022

Doctoral Committee:

Associate Professor Rhima M. Coleman, Chair
Professor David Kohn
Associate Professor Geeta Mehta
Associate Professor Ariella Shikanov

Yue Qin

qiny@umich.edu

ORCID iD: 0000-0003-2987-189X

Dedication

To my fiancé, Xuehui, who has been a limitless source of love and support.

To my family and friends, for all the sincere help and encouragement.

To Yuumi, for your companionship throughout my time in Ann Arbor.

致爸爸妈妈，外公外婆，爷爷奶奶

Acknowledgments

First and foremost, I would like to thank my thesis advisor, Dr. Rhima Coleman. I am deeply appreciative of your continual support, intellectual guidance, encouragement, and unlimited patience throughout my time in the Master's and Doctoral programs. The exceptional mentorship you provided and the precious time you spent made sure my thesis is always on track and help me develop critical thinking and independent research skills.

I am very fortunate and grateful to my dissertation committee members, Dr. Ariella Shikanov, Dr. David Kohn, and Dr. Geeta Mehta, for their support and helpful suggestions to my thesis project. Thanks for providing unique insights and valuable ideas that brought different perspectives into my work, which is paramount to the realization of this thesis.

I would like to express my special thanks to the current and former members of the CHaR lab. To Gurcharan Kaur, Ciara Davis, Dr. Tiana Wong, and Dr. Ryan Rosario, thanks for your countless help during my graduate training and moral support throughout this journey. I truly enjoyed working together with you all over the last several years.

I would also like to acknowledge the talented collaborators, Dr. Scott Hollister and Dr. Harsha Ramaraju, Georgia Institute of Technology. It has been a great pleasure collaborating with you all and I appreciate the guidance and expertise provided, helping me get started on my project.

This thesis could not have been finished without the help and support of many people who are gratefully acknowledged here.

Table of Contents

List of Figures

Abstract

Articular cartilage has a limited ability to self-repair, which often causes focal defects to progress into post-traumatic osteoarthritis. Autologous chondrocyte implantation, a process in which chondrocytes are harvested from the patient, expanded in monolayer culture, and injected into the defect, is one of the most common approaches to treating cartilage defects. However, chondrocyte dedifferentiation during this process reduces their ability to durably restore cartilage function. Chondrocyte-based cartilage tissue engineering offers alternative approaches for cartilage repair to overcome the limitations of current clinical options by developing environments that combine cues from synthetic scaffolds and biological factors to enhance chondrocyte function. However, the translation to the clinic has been limited by our incomplete understanding of how scaffold design parameters interact together to control cell function. Therefore, this dissertation focuses on designing a chondrocyte-based biomaterial platform made with a novel elastomer, poly (glycerol-dodecanedioate) (PGD), to investigate the combinatorial effects of scaffold parameters, such as surface modification and pore geometry, on chondrocyte function *in vitro*.

First, this thesis evaluates the effects of surface modification of PGD on the shape and extracellular matrix (ECM) production of chondrocytes, both of which are crucial for robust cartilage formation. Two different strategies were investigated to generate a PGD surface with enhanced hydrophilicity: 1) coating with various concentrations of collagen type I (Col I) or hyaluronic acid (HyA) individually or in combination, or 2) altering the surface charge and roughness using various levels of alkaline hydrolysis. The results revealed the combinatorial effects of ligand composition and density on human articular chondrocyte (hAC) function.

HyA-coated PGD induced a round cell shape, leading to higher ECM production, while Col I-coated PGD induced a polygonal shape. Coating with either HyA or Col I alone induced a dose-dependent response to the retention of both ligands on PGD. The combination of Col I and HyA, even with a higher HyA retention level, was not conducive to higher ECM accumulation than HyA alone. The combinatorial effects of surface charge and roughness affected hAC function in a complex manner. Increasing hydrolysis level led to higher surface charge density, however, this changed PGD's surface morphology and roughness. Slightly rough surfaces with moderately charged resulted in round cell morphology and the highest ECM production.

Lastly, this thesis describes a novel approach to generating porous PGD scaffolds with tailorable pore structures. Additionally, finite element analysis was used to determine if the local strain fields that developed inside the pores under load could be tuned to be within the range shown to have an anabolic effect on chondrocyte function. The tensile strains that develop along 31% – 71% pore surfaces inside of porous PGD scaffolds, according to varying pore size and porosity, were at levels shown to stimulate chondrocyte ECM production, indicating that the pore structural parameters could be tuned to optimize cellular strain profiles. These results suggest that porous PGD scaffolds have the potential to guide cartilage regeneration.

Overall, this dissertation presents a strategy for designing an ideal platform to support hAC redifferentiation using a novel bioelastomer, PGD. This thesis provides a reasonable approach to optimize scaffold design and investigate the mechanistic regulation of scaffold parameters on chondrocyte function for tissue engineering purposes, which will be a significant push towards clinical application of chondrocytes-based cartilage defect repair using PGD or other elastomers with similar polyester properties and nonlinear elasticity.

Chapter 1

Introduction

1.1 Thesis Motivation and Objective

Articular cartilage has a limited ability to self-repair, which often causes focal defects to progress into post-traumatic osteoarthritis (PTOA) [1]. Osteoarthritis is a disease marked by the gradual destruction of cartilage leading to pain and often disability and impacted over 300 million people in the world in 2017, with societal costs of over $15 billion per annum [2]. Traumatic injury of cartilage results in PTOA, which accounts for 12% of OA cases [1]. Currently, the clinic treatment option for cartilage defects involves microfracture, osteochondral transplantation, and autologous chondrocyte implantation. However, the current options have serious limitations and cannot fully restore cartilage function. Autologous chondrocyte implantation (ACI) is the most common approach to treat articular cartilage injuries but has multiple invasive isolation procedures and is limited by the availability and quality of donor chondrocytes [3].

Cartilage tissue engineering (CTE) has been developed to provide alternative strategies for cartilage repair that aims to overcome the limitations of current clinical options. There are three essential components of this discipline: cells, scaffolds, and biological or environmental factors, and it is the synergistic interaction among them that contribute to the functional success of an engineered cartilage construct [4]. The discipline has developed in the last several decades, yielding multiple engineered platforms with different properties, using various biomaterials and scaffold design parameters, to create a construct that restores cartilage function. However,

the translation of these new engineered materials and structures from research laboratories to the clinic has been extremely limited by our incomplete understanding of the requirements of scaffold design parameters and the roles of these parameters in targeted tissue regeneration [5]. Therefore, there is a growing need to develop platforms that are tailorable for common design parameters, such as surface properties, pore structure, and mechanical behavior in response to load. Scaffold architecture, particularly pore structure, greatly affects scaffold mechanical properties, mass transportation, and strain fields under loading, influencing chondrocytes functionality and matrix production during culture. The biomaterial and scaffold architecture design that best supports the production of articular cartilage structural macromolecules by chondrocytes remains an open, yet critical question. The properties of the scaffold surface, such as charge and roughness, also affect the cell-material interaction, making these parameters another important factor that influences matrix production. The **overall goal** of this thesis was to investigate a novel biodegradable elastomer, poly (glycerol dodecanedioate) (PGD), as a platform with easily modifiable design parameters to enhance chondrocyte-based cartilage formation. I aim to improve the overall functionality of cartilage tissue-engineered constructs created with cell-seeded elastomeric materials by modifying the scaffold design parameters. I also intend to establish a feasible design-test strategy that could help streamline the creation of new engineered scaffolds for tissue engineering aspects, by step-wisely optimizing scaffold design parameters, to ultimately support *in vitro* tissue regeneration and restore tissue function in long-term pre-clinical studies. I **hypothesize** 1) that the presentation of ECM ligand or hydrolysis treatment will enhance chondrocyte matrix accumulation and 2) that the structural geometry of the scaffold will influence its strain field under loading.

Overall, by testing our hypotheses, I engineered an elastomer platform for enhancing cartilage regeneration with various scaffold parameters of PGD, including surface properties, pore structure, and its corresponding strain field, to investigate the combinatorial influences of surface modification, i.e. ligand coating and hydrolysis on human articular chondrocyte (hAC) function and explore the influence of pore structural parameters, i.e. pore size and porosity, on the cell-level strain that develops within the scaffold under loading.

1.2 Specific Aims

1.2.1 Aim 1: To Determine the Effects of Surface Modification on Chondrocyte Function on PGD

Poly (glycerol-dodecanedioate) is a novel biocompatible and biodegradable elastomer with soft tissue-like compressive properties (rubber-like elasticity), making it a viable scaffold choice for cartilage tissue engineering. However, the surface properties of PGD are not ideal for cell growth due to its relative hydrophobicity compared to the natural extracellular matrix (ECM). Herein, I investigate two different strategies of surface modification for PGD to explore the effects of surface modification on chondrocyte function on PGD.

1.2.1.1 Aim 1a: To Determine the Effects of ECM Ligands Coating on Chondrocyte Shape and Cartilage Matrix Accumulation on PGD

The structural macromolecules of articular cartilage extracellular matrix (ECM)--collagen II, aggrecan, and sulfated glycosaminoglycans (sGAGs)--are important for the unique mechanical function of this tissue. Therefore, inducing the production of these ECM components by

chondrocytes on a scaffold is important for the successful implementation of cartilage repair strategies *in vivo*. One way that has been shown to enhance chondrocyte ECM production is the inclusion of cartilage ECM ligands on scaffolds *in vitro* [6-8]. The objective of this aim is to evaluate the effects of the type and amount of ligands on cell shape and cartilage matrix accumulation on PGD. I **hypothesized** that the type and density of ligands will impact the shape and ECM production ability of chondrocytes. In this aim, various amounts of collagen type I (Col I) or hyaluronic acid (HyA) individually or in combination was coated on the PGD film to accomplish the objective. The optimal coating protocol of collagen type I and HA was determined through qualitative and quantitative analysis of cell shape and matrix production.

1.2.1.2 Aim 1b: To determine the effect of hydrolysis treatment on chondrocytes shape and cartilage matrix accumulation on PGD

A high seeding density of the chondrocyte on scaffolds is required to promote the formation of functional cartilage tissue *in vitro*. Increasing negative charge density on the scaffold surface promotes cell attachment and ECM production, thus impacting chondrocyte function [9, 10]. Therefore, surface hydrolysis to the polymer is a good strategy to increase the hydrophilicity and cell attachment without changing the bulk properties [11, 12]. However, studies have shown the change in surface roughness and topography of polymeric scaffolds during hydrolytic surface modification, which are also crucial scaffold design parameters that impact chondrocyte behavior [13, 14]. The objective of this aim is to evaluate the effects of the hydrolysis level on cell shape and cartilage matrix accumulation on PGD. I **hypothesized** that the level of hydrolysis treatment will impact the shape and ECM produced by chondrocytes. Surface modification was achieved by sequential controlled alkaline hydrolysis and acidification of the PGD film to expose COOH functional groups on its surface. The level of

hydrolysis was controlled by varying hydrolysis time and alkaline concentration. The optimal hydrolysis profile was determined through both qualitative and quantitative analysis of cell shape and matrix production.

1.2.2 Aim 2: To Develop Porous PGD Scaffolds and Investigate the Effect of Pore Geometries on Cellular Level Strains that Developed inside the Scaffolds

Porous three-dimensional (3D) structure and interconnected pore networks are essential requirements of engineered cartilage scaffold to support extracellular matrix (ECM) production of the cell and promote nutrient and waste exchange. Cell function as well as new tissue regeneration rely heavily on the size of the pores and porosity of the scaffold [15]. Chondrocytes increase the extracellular matrix production of articular cartilage structural macromolecules in response to applied loads, therefore it is important to understand the role that scaffold plays in the stress/strain field that develops around the cells during cyclic loading. Combined pore structure and the material stiffness of the scaffold will influence the stress/strain fields that cells are exposed to under load. The objective of this aim is to develop porous PGD scaffolds with tailorable pore structure and investigate the effect of pore size and porosity on the cellular level strain field that developed inside the PGD scaffolds. I **hypothesized** that the strain fields that developed inside PGD scaffolds under loading will be controlled by managing the structural geometry of the scaffold to reach the magnitude proven to be beneficial to ECM production by chondrocytes. PGD scaffolds with tailorable, interconnected pore structures were created using an inverse molding technique. The range of scaffold structural parameters achievable (pore size and porosity) using inverse molding and subsequent mechanical properties were evaluated using microcomputed tomography (micro-CT) and compressive testing, respectively. Finite element modeling (FEM) was used to

determine the distribution of maximum tensile strain inside porous PGD scaffolds with varying pore parameters. The percentage of pore surface area that produces strain level shown to enhance cartilage ECM production in the literature was quantified, to determine the impact of pore geometries of porous PGD scaffolds on the development of cell-level strains on the scaffold pore surface under loading.

1.3 Preview of Thesis

This document is structured to provide the background and motivation for the overall dissertation project, followed by a description of the rationale, methods, results, and discussion of each of the Specific Aims in sequence. The contents of each chapter are described briefly in the following paragraphs.

Chapter 2 provides broad background information on articular cartilage tissue engineering. This chapter first introduces the fundamental information on articular cartilage, its injury, and clinic repair options. I outline the many limitations of current treatment options, which motivates tissue engineering approaches to generating cell-based cartilage grafts as a promising alternative treatment for the repair of critical-sized defects. This chapter then summarizes conventional strategies and reported challenges in cartilage tissue engineering and introduces PGD as a viable scaffold option. This chapter then summarizes common scaffold design parameters and promising techniques to modify these parameters, offering perspectives on how modifying scaffold design parameters facilitate the development of the neo-cartilage in the scaffold.

Chapters 3 and 4 focus on employing these strategies to engineer a cartilage construct using PGD and investigate the effects of scaffold design parameters on chondrocyte function.

Chapter 3 (Aim 1) investigates two surface modification approaches for PGD, Aim 1a: ligand coating and Aim 1b: surface hydrolysis, that facilitates chondrocyte attachment and ECM production. To emulate this process, human articular chondrocytes (HAC) were cultured on PGD two-dimensional (2D) surfaces with different coating or hydrolysis profiles in the chondrocyte redifferentiation medium. These chapters reveal rationales for using a surface modification to improve the biocompatibility of biomaterials and facilitate cell culture outcomes. Chondrocytes responded differently to different profiles of surface modification, which improved the understanding of the roles of scaffold surface properties in chondrocyte-material interactions. Chapter 4 (Aim 2) employs an inverse molding method that affords control of scaffold pore structure parameters (i.e., pore size and porosity). Additionally, considering chondrocyte experiences loads in a human joint, the cellular strains that developed inside porous PGD scaffold under compression were analyzed via finite element modeling. This chapter reveals both pore structure and subsequent cellular-level strain cues can be easily altered by our pore-creation strategy, which provides rationales for future scaffold design. Overall, this chapter establishes the framework for generating cartilage tissues using the proposed elastomer platform, while highlighting the need for modifying scaffold parameters in a comprehensive aspect to enhance cartilage regeneration.

Chapter 5 provides an overall summary and discussion of the results and their impact on cartilage tissue engineering, as well as a description of potential future work that could be undertaken to augment and extend the findings. This chapter summarizes and discusses key findings from this thesis and proposes future directions to fulfill the translational potential of our elastomer platform. The ability to control relevant microenvironmental cues to maximize the regenerative capacity of HAC motivates the surface modification and pore-creation approach described in this work and establishes it as an attractive scaffolding technology in cartilage repair.

Overall, this thesis presents a stepwise approach to developing *in vitro* model system using PGD to investigate the impact of scaffold parameters on the matrix-producing capacity of chondrogenic cells, while examining strategies to optimize a biomaterial-based construct for cartilage tissue engineering.

Chapter 2

Background

2.1 Articular Cartilage Injury and Repair

2.1.1 Articular Cartilage and Post-traumatic Osteoarthritis

Articular (hyaline) cartilage is the connective tissue found at the ends of long bones (**Figure 2.1**). It provides a smooth, near-frictionless surface, facilitates transmission of load, and protects the subchondral bone from the high mechanical load during joint movement. The mechanical function of articular cartilage largely relies on the specialized composition and organization of the extracellular matrix (ECM) deposited by chondrocytes [16]. Chondrocytes are the sole cell type in articular cartilage, which is sparsely distributed within a dense ECM network of their secretion (**Figure 2.2**). In the load-bearing zone of articular cartilage, the ECM composition is dominated by aggrecan and collagen type II, which mainly contribute to the cartilage's mechanical integrity (**Figure 2.2**). Collagen type II (Col II) is a fibrous protein that provides macromolecular entrapment and the tensile strength in articular cartilage to resist the swelling pressure provided by aggrecan and the tensile loads that are exerted on the cartilage during joint movement. Aggrecan is a proteoglycan that contains sulfated glycosaminoglycan (sGAG), e.g., chondroitin sulfate and keratin sulfate. sGAG is a negatively charged side chain molecule of aggrecan that attracts water from the aqueous synovial environment into cartilage tissue, therefore aggrecan has a flow-dependent viscoelastic property and offers hydrostatic swelling pressure that resists the compressive loads applied to the cartilage. The interstitial water attracted by sGAG helps to exchange nutrients with synovial fluid and lubricates the joint

and contributes to compressive resistance. Robust cartilage matrix production is usually the gold standard for cartilage regeneration outcomes, based on the important function of these matrix macromolecules.

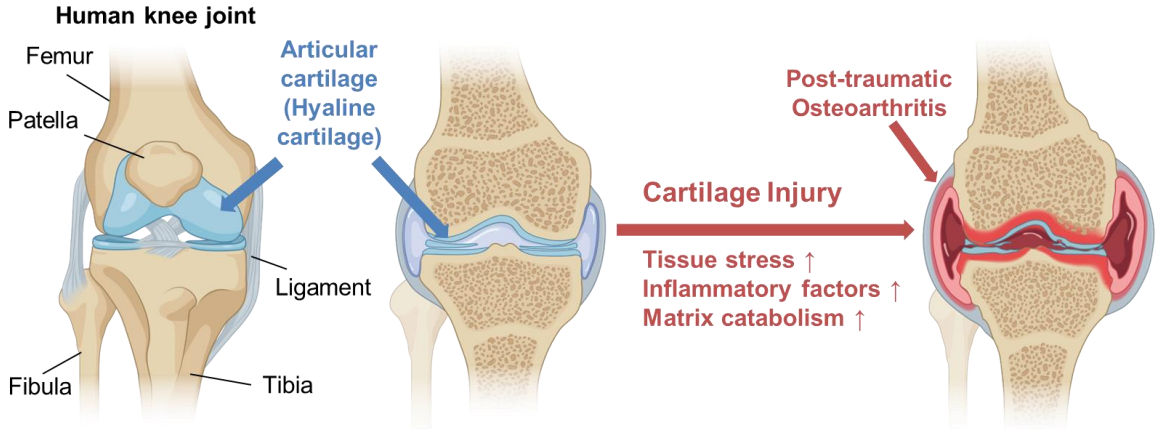

Figure 2.1 Schematic diagrams of knee joint anatomy and the progression of healthy articular cartilage to post-traumatic osteoarthritis.

Osteoarthritis (OA) is the most common joint disease marked by the gradual destruction of cartilage, leading to pain and often disability. It is impacting over 300 million people in the world in 2017 [2]. Articular cartilage lacks blood vessels and nerves, preventing the injury sites from accessing progenitor cells and nutrients so that articular cartilage has limited ability to self-repair. Traumatic injury of cartilage often leads to post-traumatic osteoarthritis (PTOA), which accounts for 12% of OA cases [2]. The disrupted tissue integrity causes abnormally high loads on the surrounding cartilage, and this excessive mechanical stress leads chondrocytes to secrete inflammatory cytokines and matrix-degrading enzymes (**Figure 2.1**), which further suppress the synthesis of aggrecan or collagen type II and result in abnormal fibrocartilage [1, 17, 18]. At this point, inflammation, matrix catabolism, bone-to-bone articulation, significant pain, and disability can be gradually developed in PTOA patients.

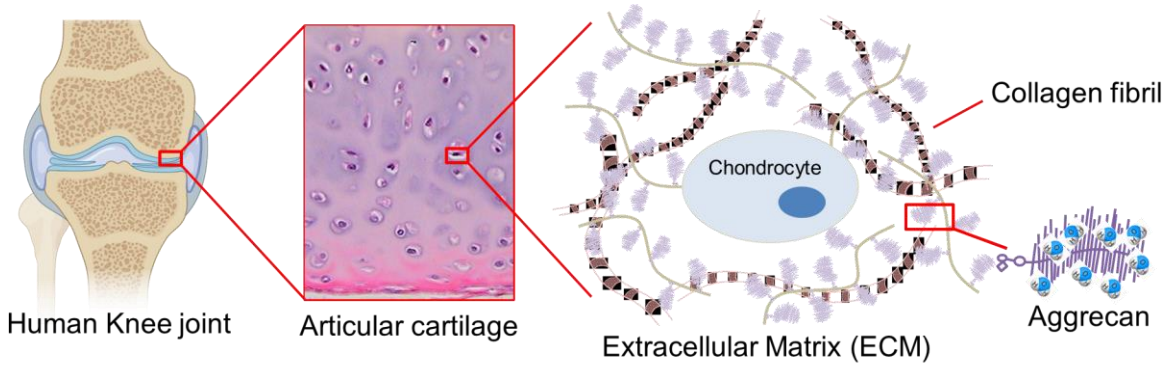

Figure 2.2 Composition and organization of the extracellular matrix in articular cartilage.

2.1.2 Current Clinical Repair Strategies for Articular Cartilage Traumatic Injuries

There are various clinical options to repair the cartilage defect and prevent further loss of cartilage. However, the current treatments all have their limitations and fail to fully restore cartilage functionality in long term.

Microfracture

Microfracture surgery is a quick, convenient, and minimally invasive method to treat smaller articular cartilage defects. During the surgery, microfractures are created in the underlying subchondral bone via drilling and shaving. Microfracture causes the subchondral bone to release bone marrow progenitor cells to set up cartilage repair. However, it should be noted that microfracture is only effective for small cartilage defect (e.g., < 2 cm^2) and the repair results has high inter-patient variability [4]. With few recruited progenitor cells or poor donor cell quality, in some cases, fibrocartilage is generated, thus resulting in further surgery and an early onset of PTOA [19-21].

Osteochondral allografts

Osteochondral allografts use cartilage tissues from tissue banks, thus avoiding the limitations

like donor site morbidity, multiple-step surgeries, and insufficient supply of donor cartilage tissue. However, it may lead to contour mismatching between the allograft and surrounding tissue and reduced load-bearing capacity, allografts may also induce immune reactions such as inflammation or rejection [4]. Lastly, allografts are often not freshly harvested and contain dead cells that cannot maintain the frictionless articular surface [4, 22, 23].

Autologous Chondrocyte Implantation and MACI

Autologous chondrocyte implantation (ACI) is a widely used treatment for osteochondral defects in the knee [3]. For ACI, chondrocytes are harvested from the non-weight-bearing zone of the joint, expanded for ~ 4 weeks in monolayer culture, and then re-implanted in the damaged region under a periosteal patch via an open joint procedure (**Figure 2.3**). However, there are limitations and disadvantages of classic ACI that cause a post-operative failure rate of 16% within 2 years [24]. For example, the multiple invasive ACI procedure has a long recovery time and considerable cost [23]. In addition, the hypertrophy and calcification caused by periosteum, dedifferentiation of chondrocytes during *in vitro* culture, and decreased human chondrocyte number with aging may impair the repair [4, 25, 26].

More recently, matrix-induced autologous chondrocyte implantation (MACI) has been adopted to overcome current limitations and improve treatment efficacy. The following generation of ACI consists of seeding chondrocytes in collagen I/III membrane, collagen matrix or engineered scaffold to replace the periosteal patch [3] (**Figure 2.3**). The most promising developments in this field involve natural or synthetic biomaterial scaffolds since it has been shown that delivery of chondrocytes with engineered scaffolds improves cartilage regeneration outcomes in cartilage defects [3, 27]. MACI is an FDA-approved treatment option involving seeding the cells on collagen membrane. The reported failure rate is reduced to 10.7% at seven years compared to the 33% failure rate in the first generation of ACI, but there are still

limitations [3]. MACI requires using *in vitro* expansion of chondrocytes in monolayer which causes chondrocyte dedifferentiation so that not creating a robust matrix. MACI also shows the inability for the implants to integrate with the surrounding native cartilage thus not fully restoring the cartilage function in the defect.

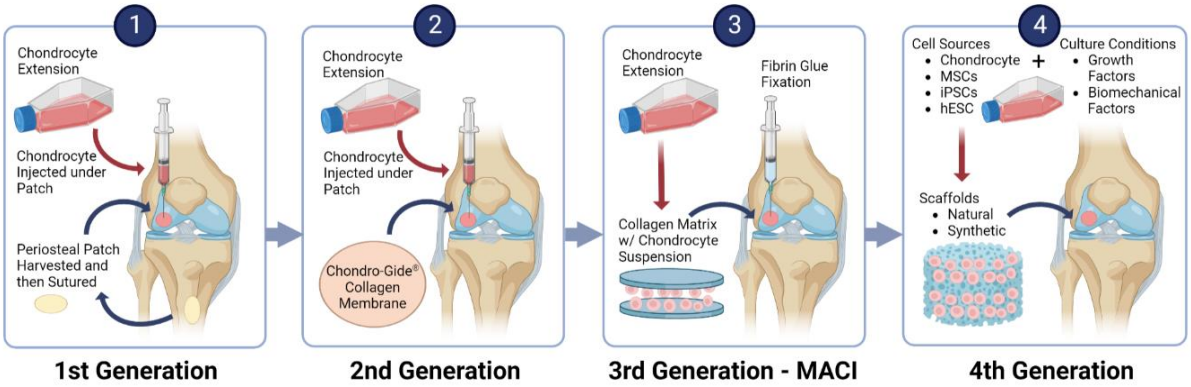

Figure 2.3 An overview of the evolution of autologous chondrocyte implantation (ACI).

ACI and MACI both require monolayer expansion of articular chondrocytes to increase the yield of cells and minimize the amount of donor cartilage tissue required. However, studies have shown that primary articular chondrocytes have limited potential to proliferate and tend to dedifferentiate during *in vitro* expansion [3]. Chondrocytes in long monolayer culture experience significant changes in their morphology and phenotype [28-32] (**Figure 2.4**). With increased passage numbers, chondrocytes produce inferior ECM upon dedifferentiation with low load-bearing ability compared to hyaline cartilage.

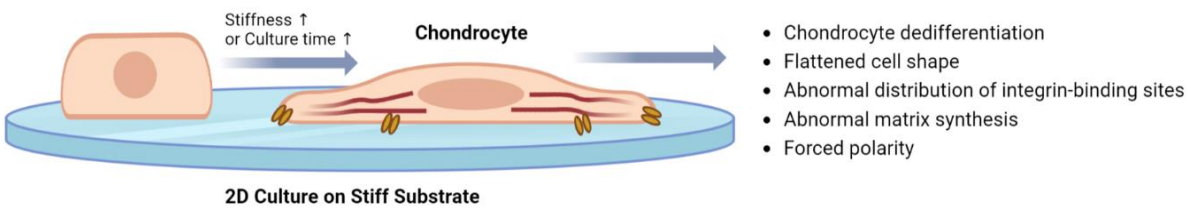

Figure 2.4 A schematic diagram of the aberrant phenotype of cell cultured on 2D stiff plastic substrates.

2.2 Cartilage Tissue Engineering

Cartilage tissue engineering (CTE) is developed to overcome the limitations of traditional treatment and provide an alternative strategy for cartilage repair. There are three essential components, also known as the "tissue engineering triad", of this discipline: 1) a biocompatible scaffold closely resembling native cartilage extracellular matrix (ECM), (2) chondrogenic cells to generate neo-cartilage, (3) biological or environmental factors that maintain desired cell function (**Figure 2.5**). The goal of *in vitro* 3D culture for cartilage tissue engineering is to reverse the chondrocyte dedifferentiation occurring in 2D expansion and achieve chondrocyte redifferentiation and maintain its phenotype in a engineered 3D environment. This required using functional cell type, engineering the scaffold with ideal design parameters, and choosing suitable culture conditions.

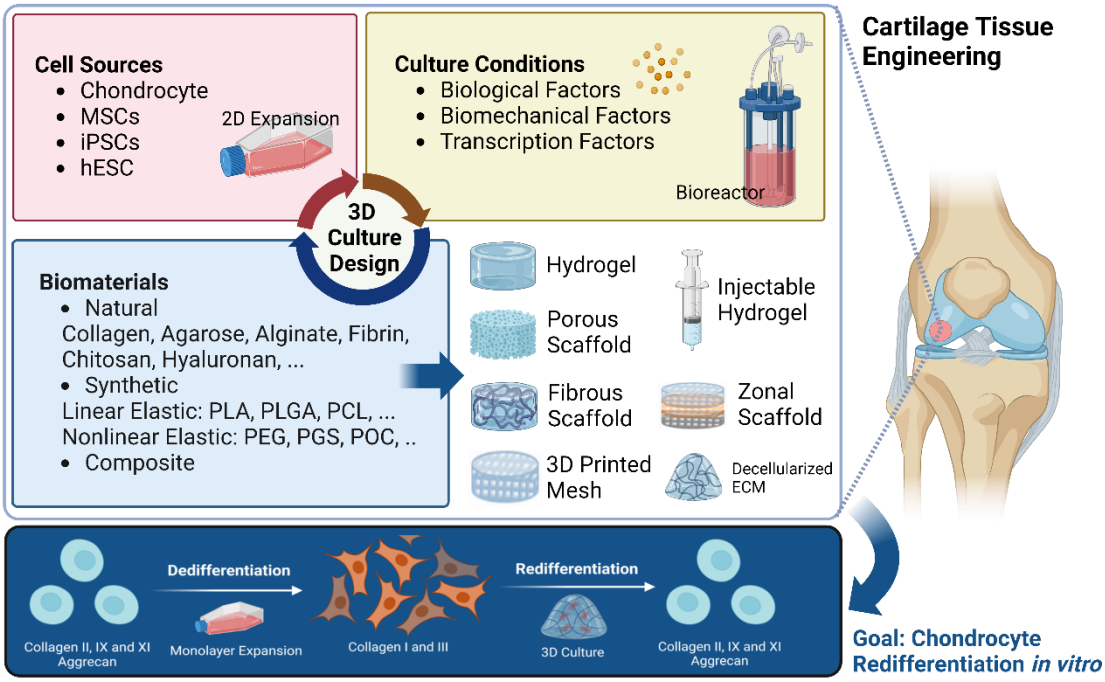

Figure 2.5 General schematic of approaches used in cartilage tissue engineering. The common approach range from numerous biomaterials and injectable systems with varying *in vitro* culturing methodologies prior to implantation [33]. The goal of *in vitro* 3D culture is to achieve chondrocyte redifferentiation and reverse the chondrocyte dedifferentiation occurring in 2D culture.

2.2.1 Cells for Cartilage Tissue Engineering

Cell-based cartilage tissue engineering is a promising strategy for cartilage repair. It involves the *in vitro* expansion of articular chondrocytes or their precursor cells which are seeded into a well-designed scaffold, for cultivation and subsequent implantation into the cartilage defect (**Figure 2.5**). Primary chondrocytes are the only type of cells that have been approved by the FDA to repair articular cartilage. The development of chondrocyte-based scaffolds and chondro-conductive culture environments has progressed significantly over the past two decades, such as work with polyglycolic acid (PGA)-fibrin scaffolds [34] and alginate hydrogels [35]. Articular chondrocyte-based repair strategies have evolved from scaffold-free implantation in ACI, to collagen membrane-immobilized delivery in MACI, and eventually to the chondrocyte-encapsulated 3D scaffolds [3]. However, the limitation in available autologous chondrocytes, immune responses to allogeneic or xenogeneic chondrocytes, and chondrocyte dedifferentiation during monolayer expansion still limits the success of chondrocyte-based treatment strategy [4, 36]. Other cell types, such as mesenchymal stem cells (MSCs), embryogenic stem cells, and induced pluripotent stem cells (iPSCs), have been examined as an alternative to articular chondrocytes for cartilage regeneration [37].

2.2.2 Scaffolds for Cartilage Tissue Engineering

Chondrocytes seeded in monolayer experience significant changes in their morphology and phenotype, which is also known as chondrocyte dedifferentiation. The makers of dedifferentiation include the shape of chondrocytes shift from round toward fibroblastic shape with culture time, the ratio of type II /type I collagen as well as aggrecan/total ECM decrease along dedifferentiation process [38]. To generate stable cartilage-like tissue for cartilage

regeneration, studies aim at optimizing cell culture approaches. Generally, efficient chondrogenic conditions involve 3D cell culture combined with the addition of chondrogenic growth factors to support chondrocyte redifferentiation (**Figure 2.5**). Common strategies for 3D chondrocyte culture involve forming a dense cell pellet, or using artificial matrices such as hydrogel (e.g., alginate, agarose or fibrin) or synthetic biodegradable scaffold (e.g., poly-glycolic acid, PGA) [38].

Scaffold is three-dimensional biomaterial which is designed to provide mechanical support and a microenvironment that facilitate cell function for cell-based cartilage tissue engineering. The scaffold for cartilage regeneration is generally required to have the following functions [5, 37, 39], which include (1) three-dimensional (3D) pore geometry for the diffusion of nutrients, (2) biocompatible material surface interface to promote cell attachment and expression of their normal phenotypes, (3) appropriate mechanical properties to induce chondrocyte-anabolic ability during the regeneration process and load-bearing ability during early implantation stage, and (4) adequate biodegradability after sufficient new cartilage formation. All those properties will meet the final goal of inducing chondrocyte redifferentiation and enhancing the quality and quantity of ECM production. The first objective of a cell-based engineered scaffold is to guide cells to generate robust ECM. During this stage, collagen type II, proteoglycan, and sGAG, as the primary matrix components in the articular cartilage ECM, have always been used as the criteria for the identification and evaluation of the chondrogenic capacity of cell-based constructs for cartilage tissue engineering. The next objective is to generate a construct mimicking the hierarchical ECM organization of nature cartilage which consists of layers of the graft with depth-dependent topographic and mechanical properties [40, 41].

2.2.2.1 Current Scaffold Choices for Cartilage Tissue Engineering

To date, a range of biomaterial scaffolds including natural materials extracted from living organisms and synthetic materials obtained from various chemical processes have been widely investigated for tissue repair and regeneration (**Figure 2.5**) [33].

Natural biomaterials are popular scaffolds for cartilage repair and regeneration due to their good biocompatibility for cell attachment and differentiation. Specifically, natural scaffolds used in articular cartilage tissue engineering include carbohydrate-based hyaluronic acid, agarose, alginate, chitosan, and protein-based collagen and fibrin hydrogel [37]. However, natural materials have limitations such as challenges in manipulating their properties, inconsistency in tissue quality due to donor variety, weak mechanical properties that fail to bear the high mechanical load exert on native cartilage, and/or poor *in vivo* degradation properties [4, 42].

The synthetic scaffold has advantages in cartilage tissue engineering such as good biocompatibility, suitable mechanical properties, the convenience of fabrication and chemical modification, and controllable biodegradability. Synthetic polymers such as polylactic acid (PLA), polyglycolic acid (PGA), and their copolymer polylactic-co-glycolic acid (PLGA) have been used for years because they are already used in FDA-approved applications. However, their degradation products lead to inflammation, which reduces their biocompatibility. Other polymers including poly(ε-caprolactone) (PCL) have also received substantial attention for articular cartilage tissue engineering. However, these synthetic polymers exhibit linear elastic behavior with moduli in the hundreds of MPa to GPa range, resulting in a mismatch of mechanical properties with surrounding cartilage tissue leading to device failure due to tissue erosion and adverse tissue remodeling [43]. Poly (octanediol-co-citrate) (POC), poly (glycerol sebacate) (PGS), and poly(glycerol-dodecanedioate) (PGD) are rubber-like biodegradable

polyester elastomers that have the mechanical properties that match the nonlinear elasticity nature of native cartilage [44-46]. All of them are made by reacting acid and alcohol monomers via condensation using high temperature and vacuum and can be degraded by hydrolysis with non-toxic and natural metabolic intermediates degradation products[47, 48]. Unlike PGS and POC, PGD is a relatively new biomaterial in the field of tissue engineering and there are no published reports on their use for cartilage regeneration.

2.2.2.2 Controllable Design Parameters of Porous Scaffolds

Porous synthetic scaffolds have played a key role in cartilage tissue engineering as an option to treat cartilage defects and damage caused by trauma. 3D scaffolds are designed to support cell attachment, proliferation, differentiation, and anabolic activity to obtain functional cartilage tissue. There are many synthetic materials and a wide range of fabrication methods being applied to make such scaffolds, with the general acceptance that these constructs should be biocompatible, biodegradable, and mechanically stable. However, the biomaterial and scaffold design that best enhances chondrocyte matrix production during *in vitro* culture remains an open, yet critical, question. Design parameters that could enhance tissue regeneration include various characteristics, such as pore size, total porosity, pore shape, pore interconnectivity, material surface chemistry, surface charge, surface roughness, effective scaffold degradability, and scaffold stiffness. This thesis focuses on discussing the following scaffold parameters: (1) porous architecture, (2) cell-surface interface, and (3) local cell-level strain field during loading (**Figure 2.6**).

Many studies have focused on the scaffold pore geometrical effects, e.g., pore size and porosity, on cartilage development. The architectural design of scaffolds, mimicking ECM, typically is a highly porous and three-dimensional (3D) structure that allows cells to accumulate and grow inside, improve mass transportation, and finally promote the organization of a 3D functional

tissue. Furthermore, with the base material modulus, the scaffold pore architecture will determine the final scaffold mechanical properties, thus porosity and pore size are key factors to be considered. However, there is no common agreement on which range of pore size or porosity is the optimal choice for cartilage regeneration. Some studies demonstrated that larger pore size (e.g. 400 μm for chitosan-based hyaluronic acid hybrid polymer fibers) significantly enhances the ECM synthesis by chondrocytes [49], while others found that chondrocytes differentiated to a greater extent into the osteogenic pathway other than the chondrogenic direction in the scaffold with the larger pore size (e.g. 300-500 μm for poly(urethane urea) scaffold) [50]. Because there are tremendous differences in the study designs or scaffold parameters of previous research that focus on the effect of pore geometry on chondrocyte behavior, including cell seeding density, material surface chemistry, material stiffness, and so on, it is necessary to consider the co-modulating effects of those parameters with pore geometry parameters to have a better understanding about the optimal scaffold design for cartilage tissue engineering.

Incorporating cartilage-specific ECM ligand presents to the surface of the scaffold can benefit cell function and ECM accumulation. For example, incorporating ECM ligands such as collagen type I (Col I) [51], collagen type II (Col II) [52], hyaluronic acid (HyA) [53], and their combination [54] have been found to enhance the anabolic ability of chondrocyte in scaffolds. Therefore, establishing the ligand coating on scaffolds can construct physiologically relevant biological cues into scaffolds to promote ECM production. Moreover, it is believed that high seeding density [55-57] or high ligand density[58] will help to maintain the round morphology of chondrocytes, which is widely accepted as a symbol of the matrix-anabolic phenotype of chondrocytes [31, 59, 60]. The processes of cells sensing ligands are clearly influenced by ligand type and density, through the interaction of integrins and cell-surface receptors. However, controlling these interactions *in vitro* to create ideal microenvironmental cues in engineered

tissues to guide chondrocyte redifferentiation has proven very challenging. These studies demonstrate the need to build an optimal scaffold system for cartilage tissue engineering, not only considering the effect of ECM coating density or ligand type on cartilage ECM production but also how those two parameters interact with each other to co-modulate chondrocyte function.

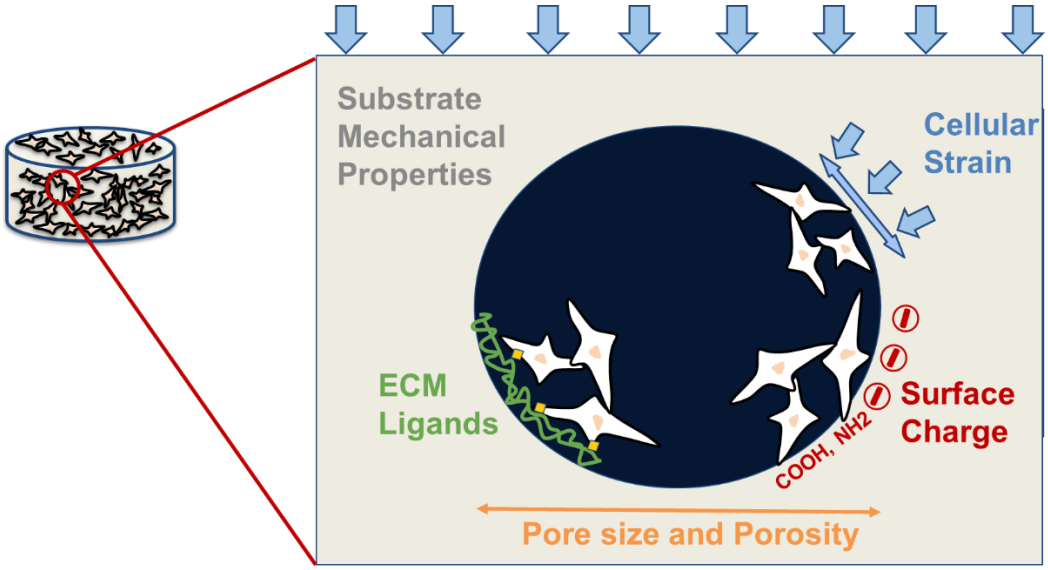

Figure 2.6 Schematic diagram of important scaffold design parameters. The design parameters in a porous polymeric scaffold that impact chondrocyte redifferentiation include pore structural parameters, ligands presentation, surface charge, material stiffness, and cell-level strain under loading. Blue arrow: the external or internal load applied to the scaffold.

Surface chemistry of the scaffold is another important parameter dictating chondrocyte function. Surface modifications such as increasing charge density and hydrophilicity promote the rounded phenotype and sGAG production in chondrocytes [10]. Studies have shown that simply increasing the number of carboxyl groups available to chondrocyte on scaffold surface increased their ECM production, suggesting surface negative charge is another parameter that can affect cell function and need to be explored [61-63]. Strategies used to increase surface negative charge (e.g., -COOH groups) for polymeric scaffold include alkaline hydrolysis, acid hydrolysis, plasma treatment, grafting copolymerization, and so on. The strategy of surface

modification for inducing -COOH groups influences other surface properties of scaffold, e.g., surface morphology and roughness. Studies have shown increasing the level of hydrolysis treatment greatly changed the surface morphology and increased ECM production by chondrocytes [13, 64], while grafting copolymerization of carboxyl group onto the surface led to no difference of surface morphology between treated and untreated polymer and worse cytocompatibility [65]. These studies demonstrate the need to investigate the interaction of those two parameters, i.e., surface charge and surface roughness, for their co-modulatory impact on chondrocyte function.

Scaffold mechanical properties that support chondrocyte ECM production under complex mechanical stresses *in vivo* are important for cartilage scaffold design [66]. Due to the presentation of integrin binding of cells to the modified surface of the scaffold, cells can sense their mechanical environment, which makes the scaffold's mechanical properties an important factor for cell function. For example, it was shown in RGD functionalized alginate scaffolds that stiffness affected not only the number of chondrocytes attached but also the arrangement of the cytoskeleton [67]. To investigate the mechanism behind this, one study confirmed ECM stiffness enhanced chondrocyte gene expression of Col2α1 and Aggrecan by promoting autocrine TGFβ1 expression on compliant substrates (0.5-MPa polyacrylamide gel) through Rho/Rho-associated protein kinase (ROCK) signaling [68]. Another study found the stiffness of the material, in this case, a silicone elastomer, polydimethylsiloxane (PDMS), affects the intercellular links among chondrocytes, such as cell−cell contact area as well as the protein level of connexin 43 (Cx43) and pannexin 1 (Panx1) [69]. Moreover, it was shown that hydrogel stiffness had synergistic effects with ligand composition on the condensation and differentiation of chondroprogenitor cells [70], which highlighted the importance of understanding the co-modulating relationship between these two parameters.

Physiological loading of cartilage produces cell deformation, which may trigger distortion of cellular structures such as the nucleus, endoplasmic reticulum, cytoskeleton, and integrins, which may then produce either direct changes in gene expression or protein synthesis that corresponds to matrix production [71]. Generally, scaffold pore size in cartilage tissue engineering is much larger than a chondrocyte, providing an environment that resembles 2D for cell attachment. Therefore, chondrocyte response to cell-level strain in monolayer potentially represents their response to the 3D environment inside the pore scaffold. A review paper summarized the influence of cyclic tensile strain on chondrocyte metabolism in monolayer culture, demonstrating loading chondrocytes between 3–10% strain led to anabolic responses while loading above 10% led to catabolic events dominated [72]. Therefore, there is a need to explore how the pore structure or stiffness of the scaffold affects the local strain field through the scaffold under load, and how the strain chondrocytes experience inside the scaffold with the same loading profile affects their matrix production during *in vitro* culture.

2.3 Poly (glycerol dodecanedioate): A Novel Elastomer for Cartilage Regeneration

Synthetic polymers such as polylactic acid (PLA), polyglycolic acid (PGA), and their copolymer polylactic-co-glycolic acid (PLGA), and polycaprolactone (PCL) have been used as a scaffold for years in the field of cartilage tissue engineering. However, these synthetic polymers exhibit linear elastic behavior and mismatch of mechanical properties with native cartilage tissue leading to device failure [43, 73]. A study has shown that elastomer (i.e., POC) with nonlinear elasticity showed higher sGAG production and lower hypertrophy after 4 weeks of *in vitro* cell culture compared to PCL, suggesting that rubber-like biodegradable polyester elastomers has the ability to support chondrocyte redifferentiation and could facilitate its function [48].

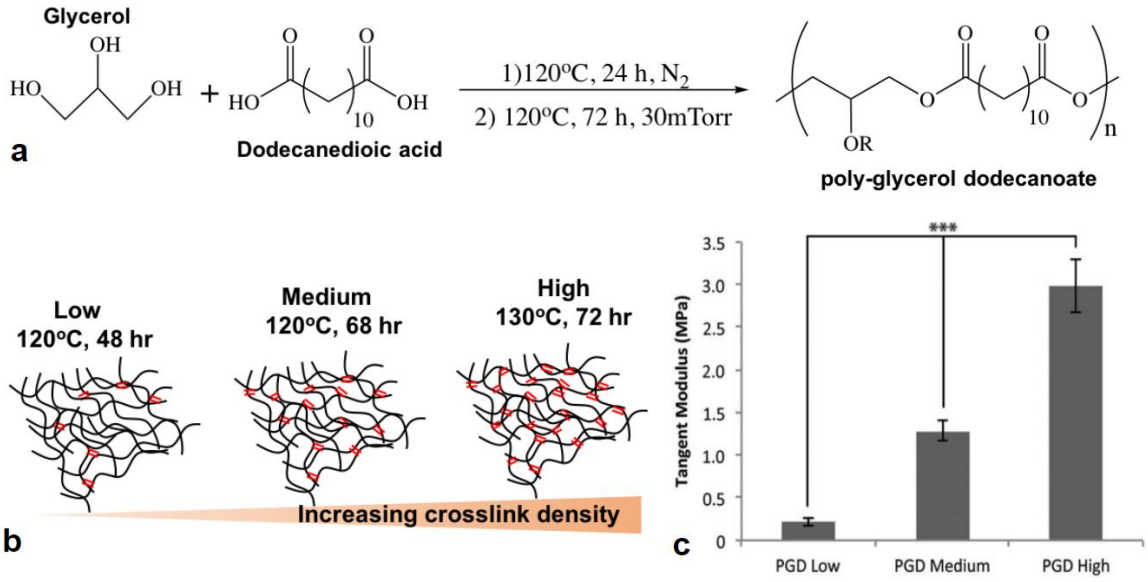

Figure 2.7 PGD material properties. (a) Reaction scheme for PGD synthesis leading to the formation of a PGD pre-polymer with R being a hydrogen bond or a carbon bond with another PGD polymer chain [74] b) Schematic of crosslink density results from varying curing conditions [74]. (c) Tangent moduli of PGD measured at 12.5% strain at 37°C (medium and high cured PGD) or 44°C (low cured PGD), *** $p \leq 0.001$ [47]. Figure adapted and used by permission from S.J. Hollister et al., 2017 & 2019.

Poly(glycerol-dodecanedioate) (PGD) is a novel biodegradable polyester elastomer formed by polycondensation of glycerol and dodecanedioic acid [46] (**Figure 2.7 a**). It was first reported in 2010 for potential use in soft tissue engineering applications to provide soft-tissue-like mechanical properties and rubber-like elasticity, slow *in vitro* degradation rate (a half-life of 16 months), shape memory behavior, and good biocompatibility [46, 47, 74]. Moreover, the crosslink density and the mechanical properties of PGD can be controlled by varying the curing time and temperature, resulting in materials with a range of moduli (**Figure 2.7 b & c**) comparable to soft tissues, like cartilage [47]. According to these properties, PGD is a viable candidate for engineered scaffold in cartilage tissue engineering. However, the application of PGD for cartilage tissue engineering is hindered by the harsh curing conditions, which limits the number of strategies that can be used to create a porous structure while maintaining the stiffness of the scaffold. Moreover, pore geometry is a crucial scaffold design parameter that

impacts the chondrocyte function in the field of cartilage tissue engineering. Therefore, a novel approach that could generate a 3D interconnected pore network in PGD and provides precise control of pore parameters, such as pore size and porosity, is urgently needed to investigate the potential of PGD as a scaffold application to the field.

2.4 Summary and Perspectives

Due to the limited regenerative capacity of the articular cartilage, focal defects in this tissue can lead to post-traumatic osteoarthritis (PTOA). There are several clinical strategies to repair cartilage defects. Microfracture is a method to recruit progenitor cells to the defect site for healing causes the development of fibrocartilage as compared to hyaline cartilage, resulting in a mismatch of mechanical properties, which compromises joint function. The use of osteochondral allografts is limited by donor site morbidity and insufficient donor tissue. In autologous chondrocyte implantation (ACI), chondrocytes are isolated, expanded *in vitro*, and implanted at the defect site to heal the defect. Although it provides good clinical outcomes in short term, this strategy is limited by chondrocyte dedifferentiation during expansion, inconsistency of donor chondrocyte quality, and heterogeneity in surgical technique. Due to the limitations of current treatments, there is a great need for regenerative treatment of cartilage injury. Chondrocytes have been applied widely for this purpose. Chondrocyte-based tissue engineering has compelling potential to overcome the limitations of current clinical options and provides a promising alternative strategy for restoring cartilage function after injury to prevent the progression of cartilage defect to PTOA. The field of cartilage tissue engineering has developed tremendous biomaterials and approaches to support cell-based therapies over decades. Polymeric scaffolds have played a key role in cartilage tissue engineering, which have functions like supporting cell attachment, proliferation, and redifferentiation, to treat cartilage

defects and damage caused by trauma. There are many synthetic materials and a wide range of fabrication methods being applied to make such scaffolds, with the general acceptance that these constructs should be biocompatible, biodegradable, and mechanically stable. However, the biomaterial and scaffold design that best enhances chondrocyte matrix production during *in vitro* culture remains an open yet critical question. To achieve adequate robust cartilage ECM in the engineered scaffold, both prior to and after implantation of the construct into the cartilage defect, a scaffold is required to provide the microenvironment cues that lead chondrocytes to undergo redifferentiation during the co-culture. This remained a significant obstacle to the long-term success of these approaches. Scaffold design parameters that could impact chondrocyte function and cartilage regenerative outcomes include pore size, porosity, surface chemistry, surface charge, surface roughness, scaffold stiffness, and so on. Therefore, the creation of constructs with tailorable design parameters is required to have a better understanding of the effects of scaffold parameters on chondrocyte function. Besides that, investigating the interactions of different scaffold parameters are also required to better understand the effects of the scaffold's environmental cues on chondrocyte phenotype and function and help to achieve an ideal scaffold design. Poly (glycerol-dodecanedioate) is a novel biodegradable elastomer that has shown good potential in scaffold design for cartilage tissue engineering [46, 47, 74]. Taken together, the field provides a solid knowledge foundation to guide the design of a scaffold with ideal parameters to provide the chondrocyte with beneficial environmental cues that help them to redifferentiation and produce a robust cartilaginous matrix.

Chapter 3

Effect of Surface Modification of PGD on Chondrocyte Function

3.1 Abstract

Prolonged monolayer expansion of chondrocyte is a necessary process for clinic treatment of large cartilage defects during an autologous chondrocyte implantation procedure. Chondrocytes undergo dedifferentiation when cultured for long period on tissue culture plastic, leading to a reduction in the quality of the matrix synthesized by the chondrocytes upon redifferentiation. Poly(glycerol-dodecanedioate) (PGD) is a viable candidate for scaffold design in cartilage tissue engineering. However, the surface properties of PGD are not ideal for cell attachment and growth due to its relative hydrophobicity compared to the natural ECM. In this Aim, this thesis evaluates the effects of surface modification of PGD on chondrocyte function. I investigated two different strategies to generate a biomaterial surface with high cell affinity: 1) coating with various concentrations of collagen type I or hyaluronic acid individually or in combination, or 2) altering the surface charge and roughness using various levels of alkaline hydrolysis. By comparing the cell shape and ECM production on PGD under various 1) ligand profiles or 2) hydrolysis conditions, I demonstrated the combinatorial effects of ligand composition and density or surface charge and roughness on human articular chondrocyte function.

3.2 Introduction

Porous synthetic scaffolds have played a key role in cartilage tissue engineering to treat cartilage defects and damage caused by trauma. Like the extracellular matrix (ECM) in natural cartilage, these scaffolds support cell attachment, proliferation, and differentiation. The overall function of a scaffold depends on many scaffold parameters (**Figure 2.6**), and among those, one of the most crucial parameters is the surface interface, which directly regulates the microenvironmental cues presented by the scaffold and thus guides chondrocyte redifferentiation. There are many synthetic materials and a wide range of fabrication methods being applied to make such scaffolds, with the general acceptance that these constructs should be biocompatible, biodegradable, and mechanically stable. Though there are lots of engineered constructs made by biomaterials that satisfy the above requirements, the design of scaffold surface interface that optimally enhances chondrocyte matrix production during *in vitro* culture remains an open, yet critical question. Moreover, the translation of these engineered grafts to the clinic has been limited by our incomplete understanding of how scaffold surface parameters interact together to control cell function. The surface parameters that could enhance tissue regeneration such as ligand-coated profile, material surface chemistry, hydrophilicity, cell affinity, biocompatibility, charge, and roughness. Herein this thesis focuses on the following scaffold parameters: ligand composition and density, or surface charge and roughness, to investigate the combinatorial effects between those parameters on chondrocyte redifferentiation.

The ECM interacts with chondrocytes through a variety of receptors to modulate chondrocyte metabolism and phenotype. Integrin attachment of chondrocyte to ECM ligand, such as collagen (via $\alpha 1\beta 1$ integrin), has been implicated in the growth factor receptor activity and transduction of mechanical signals in chondrocytes, which cause changes in intracellular

pathways and cell morphology, thus affecting cell genotype and phenotype [51, 52]. Scaffolds composed of ECM ligands may create an environment that can preserve the normal phenotype of cells to promote the regeneration of cartilage-like constructs.

The ECM ligand-presented 2D surface can benefit cell function and ECM accumulation. High density (5 mg/mL) of collagen type I (Col I) substrate in monolayer culture-maintained chondrocytes in a more rounded shape compared to a plastic substrate when the chondrocytes were seeded at low density (1×10^4 cells/cm^2) [51]. The expression of GAGs and collagen type II (Col II) were higher in cells isolated from Col I substrate than in plastic substrate after 3D culture [51]. However, another study showed that the ECM protein substrates (e.g. 0.5 mg/mL collagen type I and collagen type II did not significantly alter the changes in chondrocyte morphology, gene expression, matrix formation, or cytoskeletal organization when chondrocytes were seeded at low density (2×10^4 cells/cm^2) on these surfaces in monolayer culture [52]. The results from another study examined the effect of Col I coating on chondrocytes function, using low coating density (0.125 mg/mL) and high cell seeding density (3.8×10^5 cells/cm^2), but no significant differences in matrix production results between collagen types I and II were observed [75]. Although it is not an articular cartilage-specific ligand, these studies show that culture on Col I does have anabolic effects on chondrocyte ECM production [51, 75].

Another key articular cartilage-specific ECM ligand, hyaluronic acid (HyA), regulates chondrocyte function through interaction with the cell surface receptor CD44. HyA has a positive influence on a large number of cellular pathways including phenotypic regulation [53] and, when combined with collagen I in hydrogels, it stabilizes chondrocyte phenotype and increases proteoglycan synthesis [54]. Therefore, establishing a coating of HyA and/or Col I can be essential to incorporate more physiologically relevant biological cues into scaffolds for

promoting ECM production. Anecdotally, it is believed that high ligand density [58] will help to maintain the round morphology of cells, which is widely accepted as a symbol of the matrix-anabolic phenotype of chondrocytes [31, 59, 60]. This means that, in addition to ligand composition, ligand density is another important scaffold design parameter to consider for cartilage regeneration strategies.

The surface properties of polymeric scaffolds are sometimes not ideal for cell attachment and growth due to the material's hydrophobicity. Surface modifications such as increasing charge density and hydrophilicity promote the rounded phenotype and desired increase in sGAG production by chondrocytes [10]. Studies showed glass surfaces modified with carboxyl (-COOH, negative) functional groups induced chondrocytes to produce a higher amount of collagen type II and lower amounts of Runx2 than unmodified surfaces or positive -NH_2 functionalized surfaces [76]. Another study has shown acid hydrolysis of polyester poly(glycolic acid) (PGA) fibers improved their biocompatibility both *in vitro* and *in vivo* [11]. Presenting high cell seeding density on scaffolds can promote the formation of a cartilaginous matrix *in vitro*. Alkaline hydrolysis of PGA mesh was seeded with more than twice as many cells as unmodified PGA mesh, without significantly changing the molecular weight and thermal properties of the polymer [77]. Therefore, increasing negative charge density on the scaffold surface promotes cell attachment and induces chondrocyte redifferentiation, and hydrolysis is a viable way to achieve the charged surface of polyester scaffold without changing its mechanical properties. However, studies have shown the change in surface roughness, wettability, and topography of polymeric scaffolds during alkaline or plasma treatment due to hydrolytic surface degradation [13, 14]. Enhanced surface roughness and hydrophilicity were proven to improve the expression level of cartilage-specific genes and the production of sulfated glycosaminoglycans (sGAG) of porcine articular chondrocyte on porous poly(ε-caprolactone) (PCL) scaffolds [78]. Therefore, the magnitudes of surface roughness and

hydrophilicity changed during the surface modification, i.e., hydrolysis, of the scaffold are also crucial parameters to be considered.

Herein, I developed two different strategies by 1) creating an ECM ligand-presenting environment (Aim 1a) and 2) modifying the charge density and roughness of the surface (Aim 1b) to generate a biomaterial surface with enhanced cell affinity and ECM-anabolic ability using PGD. The cell shape and ECM production of human articular chondrocyte (hAC) were evaluated to investigate the combinatorial effects of surface modification parameters. In Aim 1a, we hypothesize there is a combinatorial effect of ligand composition and ligand density on chondrocyte cell shape and ECM production. In Aim 1b, we hypothesize increasing negative charge density and surface roughness will promote the rounded phenotype and facilitate sGAG production of chondrocytes.

3.3 Methods

3.3.1 PGD Fabrication

Prepolymer and curing

PGD prepolymer was synthesized and then cured following methods described by Solorio et al [47]. Briefly, PGD pre-polymer was synthesized by mixing glycerol and dodecanedioic acid with a 1:1 molar ratio at a 120 °C flask under nitrogen and stirring conditions for 24 h. The viscous pre-polymer was then cast into silicone molds and transferred into a vacuum oven at 130 °C for 48 h. A vacuum was pulled and maintained at 90 mTorrs for the duration of the curing process, to get the solid nonporous PGD blocks.

PGD film fabrication and preparation

PGD films were used to determine the morphology, metabolic activity, and ECM production of human articular chondrocytes (hACs) in monolayer settings. PGD prepolymer was synthesized as described above and then was cast onto positively changed microscope slides (InkJet Plus Microscope Slides, Fisherbrand) or 3 mL glass vials (Restek Corporation). The PGD prepolymer spontaneously spread to a flat surface on the positively charged glass slides or formed a flat surface on the bottom of glass vials (**Figure 3.1**), and then both were cured with the same condition as described above. All the PGD films were soaked in the growth media for 7 days with three media changes to remove any possible cytotoxic PGD byproducts that could dissolve in the media.

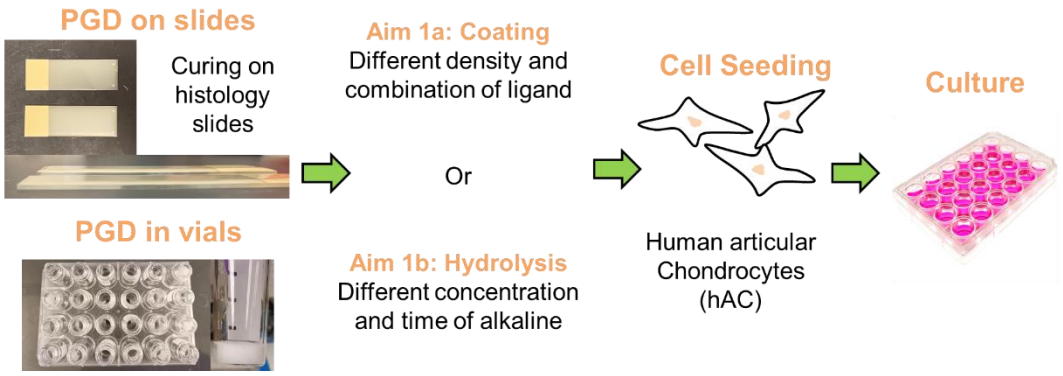

Figure 3.1 Experimental design of Aim 1. Aim 1a: PGD surface was coated by different protocols of ligands. Aim 1b: PGD surface was treated with different profiles of alkaline. Both sub-aims used the same methods for PGD fabrication, cell seeding, and *in vitro* culture conditions.

3.3.2 PGD Surface Modification

Aim 1a: Ligand coating

PGD films were coated with the ECM ligands collagen type I (Col I) or hyaluronic acid (HyA), via physical absorption. Briefly, 50 mg HA powder (MW ~1.5 mDa, Lifecore) was dissolved in a sterile 10 ml PBS solution to achieve a stock concentration of 0.5 % (w/v). Col I from rat

tail tendon dissolved in 0.1 M acetic acid solution (Corning) was purchased for a stock concentration of 0.1 % (w/v). A serial final mass of Col I or HyA on PGD was made from diluting sterile filtered stock solution (**Table 3.1**). The aqueous solution of HyA or Col I (1 ml) was pipetted onto the PGD film surface in a 4-well slide dish (Nunc rectangular dish, Thermo Scientific). All samples were air-dried for 3 days at room temperature to prepare the coated substrates. We then used a layer-by-layer strategy to coat the combination of Col I (first layer) and HyA (second layer) to improve HyA retention levels before seeding the cells.

Aim 1b: Hydrolysis treatment

PGD films were treated with varying alkaline concentrations with varying treatment times. Briefly, PGD films were immersed in the solution of 0.1 M, 0.5 M, or 1M NaOH for 5 min, 15 min, 30 min, or 60 min at room temperature, and then followed by immersed in 0.01 M HCl for 30 s to allow the transformation of ester groups on the surface of PGD to carboxylic acid and hydroxyl groups. All samples were washed with DI water and air-dried until future use.

Table 3.1 Mass of ligand coating with various coating compositions

Ligand Labels	***Mass on PGD (μg)***
C: Col I, Collagen type I	50, 100, 200, 400
H: HyA, Hyaluronic acid	62.5,125, 250, 500
C+H: First layer of C, then last layer of H	C: 200, H: 250, 500

3.3.3 PGD Surface Characterization

Aim 1a: Ligand coating

Ligand Retention Level

Coated PGD samples in vials were first immersed in 1 mL phosphate-buffered saline (PBS) at

37 °C for 24 h, and then the supernatant solution was collected to run gel permeation chromatography (GPC). Standard Col I and HyA solutions varying in concentration were prepared in PBS. Gel permeation chromatography was carried out using a refractive index detector. Both supernatant samples and standard solutions are run through the column at a flow rate of 0.6 mL/min. Col I eluted around the 9 – 10 min mark, while HyA eluted around the 7 – 12 min mark, and the total run lasted 20 min. The peak area associated with each eluting peak was quantified to calculate the concentration of Col I or HyA in the supernatant solution, represented by C_{elute}. The ligand retention level was calculated by the following equation, where $C_{initial}$ represented the initial coating concentration. The ligand retention level was also known as the mean coating efficiency of each ligand, representing the percentage of ligand remaining on the PGD surface after PBS immersion.

$$\text{Ligand retention level} = \text{Coating efficiency} = \frac{C_{initial} - C_{elute}}{C_{initial}} \times 100\%$$

Aim 1b: Hydrolysis treatment

Percentage Mass Loss

The percentage mass loss of the hydrolyzed PGD samples was tested by weighting the dry PGD samples before and after hydrolysis treatment. The percentage mass loss was calculated by the following equation, where M_{before} represented the initial weight of PGD samples, M_{after} represented the weight of treated PGD samples after hydrolysis.

$$\text{Percentage Mass loss} = \frac{M_{before} - M_{after}}{M_{before}} \times 100\%$$

Water Contact Angle

The apparent water contact angle of the hydrolyzed PGD samples was tested by a DSA100 type Contact Angle Meter (German, Gumbo Ham bur). The water contact angle was measured by depositing 5 μl of an ultrapure water droplet on the PGD surface. The angles of water droplets on the material surfaces were determined immediately.

Surface Charge

The film's surface chemical composition, i.e., surface charge, was characterized via infrared spectroscopy. Fourier transform infrared (FTIR) spectra were obtained using a Nicolet 5700 (equipped with attenuated total reflectance module, Nicolet Co., USA) with a resolution of 4 cm-1 over the range of 800-4000 cm-1. The relative amount of -COOH groups was quantified by subtracting the peak area of FTIR spectra between the untreated control group and hydrolyzed group.

Surface Topography and Surface Roughness

The surface morphology of hydrolyzed PGD samples was characterized by scanning electron microscopy. PGD samples were spray-coated with a 10-nm-thick layer of gold (Leica EM ACE200, Germany) prior to being observed on a field emission scanning electron microscopy (JSM 7800F, Japan).

The surface morphology of PGD was then recorded by MultiMode 8-HR atomic force microscope (Bruker, USA) in tapping mode using an NCHV-A Bruker AFM probe with a resolution of 512 × 512 pixels. The roughness average (Ra) was calculated by the arithmetic average of the absolute values of surface height deviation from the mean line, recorded within the 30 μm × 30 μm rectangle area of each sample.

3.3.4 Cell Seeding and Culture Conditions

Surface-modified PGD were sterilized with sterile 70% ethanol through 30 min ultrasonic wash and then overnight wash before the cell experiments. Human articular chondrocytes (hACs) from a healthy young male donor (age 19, CELLvo, StemBioSys) were expanded in the growth media: Low glucose DMEM (Gibco) supplemented with 10% FBS, 1% Antibiotic-Antimycotic, 1 ng/ml TGF- β1, 10 ng/ml PDGF-BB, and 5 ng/ml FGF-2, until the plate reached confluency. The hACs were seeded with a seeding density of 1×10^6 cells/cm^2 onto the top surface of PGD in the 4-well slide dish or 3 mL glass vials and then incubated for 3 h for cell subsidence (**Figure 3.1**). Redifferentiation medium (6 ml per well) was then added into a 4-well dish, which was formulated as high glucose DMEM (Gibco), 10% FBS, 1% Anti-Anti, 1% ITS +Premix, 10 ng/ml TGF- β1, 1.25 mg/ml BSA, 40 μg/ml L-Proline, 50 μg/mL ascorbic acid 2-phosphate, 1 mM sodium pyruvate, 100 nM dexamethasone, 10mM HEPES. The hAC-seeded PGD were then cultured in the humidified incubator (37°C, 5% CO_2) for 2 or 28 days.

3.3.5 Cell Attachment Analysis

Aim 1a: Ligand coating

To analyze the effects of ECM ligands coating on cell attachment and cell shape, hACs were seeded onto PGD flat films coated with 0.1% (w/v) Col I or 0.5% (w/v) HyA, or without coating (control group), and then were cultured for 2 days as described above. The PGD films were then examined by F-actin staining using Phalloidin TRITC (Sigma) following the manufacturer's instruction and images of hACs were taken from the fluorescence microscope or Nikon A1 Confocal. Briefly, the samples were fixed with 10% neutral buffered formalin for 30 min, were permeabilized with 0.5% TBS TX-100 for 5 min, and then were blocked with 10% Goat serum, 1% BSA in 0.1% TBST for 1 hour at room temperature. The samples were strained

with 300nM phalloidin solution for 30 min and then were sealed by coverslip with one drop of anti-fade mounting medium. Between each step, the samples were washed in 1X-TBS for 5 min. To assess cell attachment, the perimeter and area of each human articular chondrocyte were quantified by analysis of the images via ImageJ. The circularity of each cell is defined by the following equation

$$Circularity = \frac{4\pi \times Area}{Perimeter^2}$$

Aim 1b: Hydrolysis treatment

Similar to Aim 1a, hACs were seeded onto hydrolyzed or untreated (control group) PGD films, and then were cultured for 2 days as described above. Samples were then examined by F-actin, nucleus, and focal adhesion protein staining using Phalloidin TRITC, DAPI, and Vinculin monoclonal antibody (VLN01, MA5-11690), separately following the manufacturer's instruction and images of hACs were taken from the fluorescence microscope or Nikon A1 Confocal.

3.3.6 Metabolic Activity Analysis

Chondrocyte metabolic activity was analyzed via Cell Counting Kit-8 (CCK-8, Dojindo, Japan). Briefly, hACs seeded on PGD films were cultured in glass vials in 28-day culture. One hundred microliters of CCK-8 solution were added to each vial on days 2, 5, 8, 12, 15, 20, 25, and 28 and the vials were incubated at 37 °C for 4 h. The absorbance of the solution in each vial was measured at 450 nm.

3.3.7 ECM Production Assay

To analyze the effect of ECM ligands coating on sulfated glycosaminoglycans (sGAG) production, 1,9-dimethyl methylene blue (DMMB) assay was conducted on hAC-seeded PGD films cultured in glass vials after 28-day culture as previously described [45-46]. Matrix was digested with papain [45]. The absorbance was measured at 525nm and 595 nm and compared to chondroitin sulfate standards [46]. Meanwhile, the PicoGreen double-stranded DNA assay (Invitrogen) was conducted on hAC-seeded PGD films cultured in glass vials after 28 days to analyze the number of cells. The absorbance was measured at excitation at 498 nm and emission at 528 nm compared to DNA standards

3.3.8 Statistical Analysis

Unless indicated otherwise, results were analyzed using a one-way ANOVA and Tukey post-hoc test for multiple comparisons in GraphPad Prism 8.0 (GraphPad Software, San Diego, CA). The cell area, circularity, and/or sGAG production of hAC cultured on PGD film were compared across different coating groups or hydrolysis groups. The criterion for statistical significance was $P < 0.05$ in all tests.

3.4 Results

3.4.1 Aim 1a

3.4.1.1 ECM Ligands Coating Composition Influenced Chondrocyte Shape and ECM Production

F-actin staining was conducted to evaluate the influence of ligand coating on cell shape. HACs attached and proliferated on PGD films, indicating good cytocompatibility of PGD (**Figure 3.2 a & b**). The cell number was lower on non-coated PGD films than the coated ones and cell morphology was altered by the ligands. The Col I and HyA coated groups had larger cell numbers with 100% confluency and dense, multi-layered structures of cells, while the control group showed fewer cells with spaces between cell clusters resulting in a honeycomb-like structure. This suggests that ligand coatings improved hACs proliferation or attachment. HyA-coated PGD film retained more hACs with a round cell shape compared to the Col I-coated group. hACs grown on collagen type I surface had a flat, stretched polygonal shape with high numbers of stress fibers. In the HyA group, cells were smaller and rounder, and the actin fibers were distributed evenly beneath the cell membrane, which is associated with the maintenance of the chondrocyte phenotype. This was supported by quantification of cell area and circularity via imageJ analysis (**Figure 3.2 c & d**) which showed that Col I coating on PGD film increased hACs spreading, with a cell shape profile with the largest cell area and lowest circularity on Day 2, while HyA coating maintained the smaller and rounder cell shape that were typically found in 3D culture.

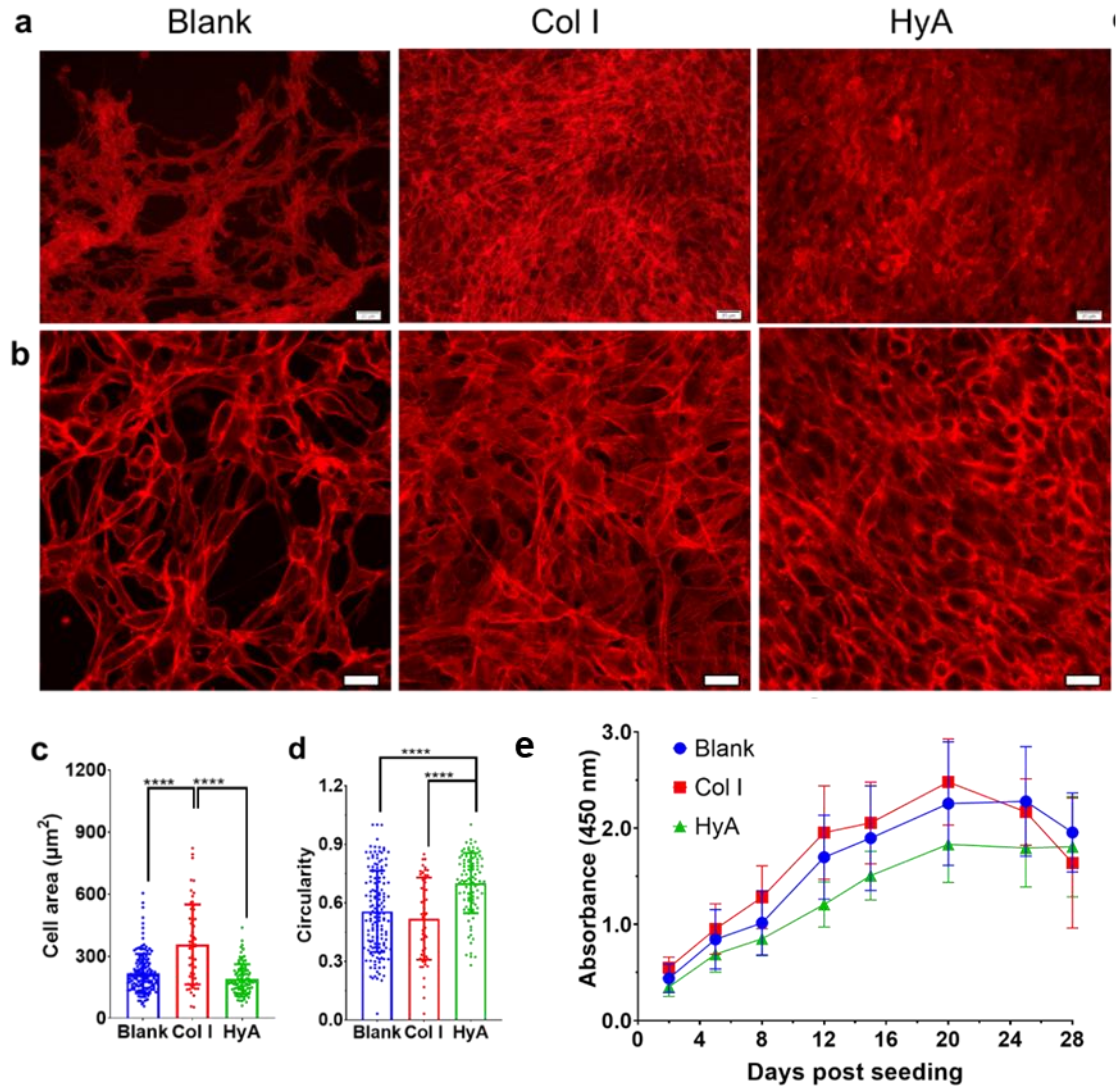

Figure 3.2 ECM ligands composition influenced chondrocyte behavior on PGD. (a) Fluorescence images of phalloidin TRITC staining (F-actin, red) on chondrocytes-seeded PGD flat films with no coating (Blank), 0.1% Col I coating (Col I) or 0.5% HyA coating (HyA) after 2 days of culture. The cell density was higher on PGD films coated with cartilage-specific ligands on Day 2. Magnification: 20X. Scale bar: 20 μm. (b) Confocal images of phalloidin TRITC staining (F-actin, red) on chondrocytes-seeded PGD flat films with no coating (Blank), 0.1% Col I coating (Col I) or 0.5% HyA coating (HyA) after 2 days of culture. The proportions of chondrocytes with round morphology were different when PGD film had different coating profiles. Magnification: 40X. Scale bar: 20 μm. (c) Quantification of the area of each chondrocyte by image analysis of F-actin staining. Data represented as mean ± s.e.m. Significant difference among Blank, Col I, and HyA is indicated by *** $p<0.001$, **** $p<0.0001$ by one-way ANOVA corrected with Tukey's multiple comparison method. (d) Quantification of the circularity of each chondrocyte by image analysis of F-actin staining. Data represented as mean ± s.e.m. Significant difference among Blank, Col I, and HyA is indicated by **** $p<0.0001$ by one-way ANOVA corrected with Tukey's multiple comparison method. (e) Metabolic activities of hACs on PGD films with different coatings in 28-day culture. Data represented as mean ± s.e.m.

The impact of ECM ligand coating on hACs metabolic activities and ECM production in 28-day culture were then analyzed. The metabolic activity of hACs in all groups increased in 28-day culture, indicating good cytocompatibility and support for cell growth. hACs cultured on

Col I-coated PGD films had the highest metabolic activity, while those on HyA-coated PGD films were the lowest (**Figure 3.2 e**). hACs cultured on Col I-coated PGD films had significantly decreased metabolic activity on day 28 compared to day 20, while hACs cultured on HyA-coated PGD films maintained their metabolic activity level on day 20 up to day 28. hACs cultured on uncoated PGD had a stable level of metabolic activity from day 20 to 24, which decreased by day 28. There were no significant differences in the metabolic activity between the three groups on day 28. The metabolic activity of hACs cultured on Col I-coated PGD films decreased between day 20 and day 28 but remained constant in the HyA-coated group.

3.4.1.2 Combinatorial Effect of Ligands Composition and Density on Chondrocyte ECM Production

According to the GPC analysis of different coated PGD samples, approximately 90% Col I or 25% HyA remained on PGD after 24 hours of immersion in PBS (**Figure 3.3 a)**. The mean coating efficiency of each ligand represented the percentage of ligand remaining on PGD surface when coated alone, after 24 h immersed in PBS, as known as ligand retention level. Combined Col and HyA (C+H) by layer-by-layer coating increased HyA retention level to above 50% (**Figure 3.3 a**).

Analysis of sGAG production highlighted the combinatorial effects of ligand composition and density on chondrocyte ECM production on PGD. There were significant differences in sGAG production levels between the different initial densities of HyA, supporting that ligand density of HyA impacted hAC anabolic activity in 28-day cultures (**Figure 3.3 b**). Higher HyA initial coating density resulted in enhanced robust ECM production. Chondrocyte ECM production

on Col I-coated PGD was highest on surfaces initially coated with 200 μg (**Figure 3.3 b**). Combined collagen and hyaluronic acid by layer-by-layer coating method resulted in different effects on ECM production compared to the individual. With the same initial density of HyA, C200+H500 group showed significant lower sGAG production than H500 group (**Figure 3.3 b**). However, C200+H250 group showed no significant difference on sGAG production compared to H250 group (**Figure 3.3 b**). Overall, we found a high density of hyaluronic acid significantly increases sGAG synthesis, and the addition of Col I significantly reduced sGAG production.

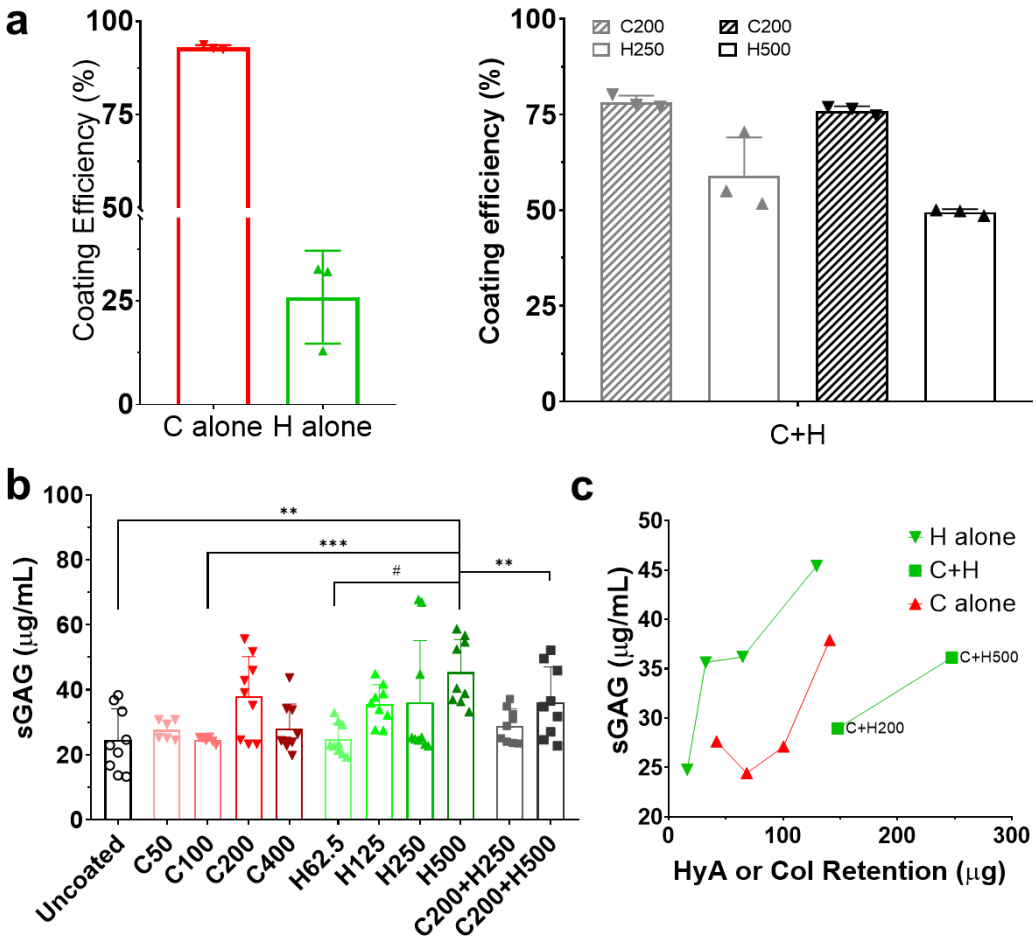

Figure 3.3 ECM ligands composition and density co-modulated ECM production on PGD. (a) Ligand retention level of various ligand compositions after 24h immersion in PBS. Data represented as mean ± s.e.m. C200: there was 200 μg Col I coated on PGD before immersion. H250 or H500: there was 250 μg or 500 μg HyA coated on PGD before immersion. (b) sGAG production of hACs on PGD films with different coatings in 28-day culture. Data represented as mean ± s.e.m. Significant difference is indicated by ** $p<0.01$, *** $p<0.001$, # $p<0.0001$ by one-way ANOVA corrected with Tukey's multiple comparison method. (c) Correlations between ligand profile and ECM production. x-axis: ligand retention level.

We then determine the correlation between ligand retention level and ECM production (**Figure 3.3 c**). There was a dose-dependent response to the exposure of hyaluronic acid or Collagen type I to hAC grew on coated PGD. Generally, HyA-coated PGD had a higher sGAG production than Col I coated and Col I + HyA combined coated PGD, despite ligand coating density. However, with similar ligand retention levels, HyA alone had larger effect on improving sGAG production compared to other combinations, suggesting higher binding efficiency does not necessarily induce higher ECM production, which supported the combinatorial effect of both ligand composition and density on chondrocyte ECM production on PGD.

3.4.2 Aim 1b Results

3.4.2.1 Alkaline Hydrolysis Regulated Surface Properties of PGD

The composition of functional groups on the surface of various hydrolyzed PGD was comparatively evaluated by Fourier transform infrared spectroscopy (FTIR). We found that increasing the level of hydrolysis resulted in an increasing amount of negative surface charge (**Figure 3.4**). FTIR spectrum confirmed successful PGD synthesis as all characteristic peaks matched the previous report of PGD material, including –C-H stretch for methylene groups at 2915 cm-1 and 2848 cm-1, and C=O stretch for ester bonds at 1730 cm-1 [46] (**Figure 3.4 a**). Treatment with different levels of alkali hydrolysis did not significantly change the intensity of these peaks representing backbone chemistry. However, due to the ester bond breakage after hydrolysis resulting in the exposure of more carboxyl and hydroxyl groups on the surface of the PGD material, we observed an increase in the intensity of the corresponding asymmetric COO- stretch at 1560 cm-1 and -O-H stretch for hydroxyl groups at 3200 cm-1 (**Figure 3.4 a**).

More specifically, after integrating the peak area of the asymmetric COO- stretch at 1560 cm-1, there was a positive correlation between its integrated area and the intensity of hydrolysis (**Figure 3.4 b**), indicating that more intense hydrolysis conditions can induce more carboxyl groups to be exposed on the surface of the PGD material. It was noted that different alkaline treatment conditions had similar relative amounts of -COOH groups, such as untreated, 0.1M-5 and 0.1M-15; 0.1M-30 and 0.5M-5; 0.5M-15 and 1M-15, allowing us to inspect the effect of surface roughness independently to surface charge on hAC function.

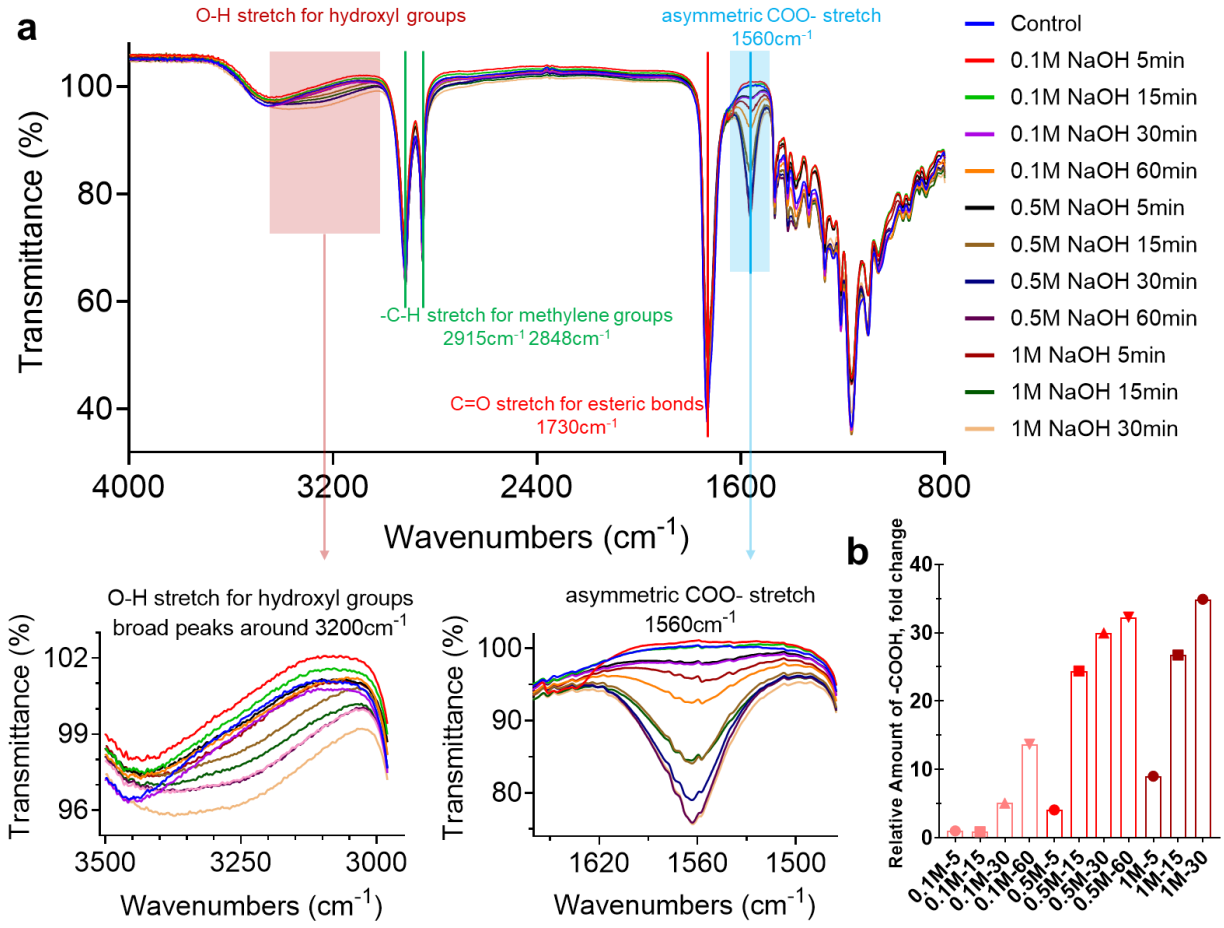

Figure 3.4 Hydrolysis level increased the surface charge of PGD. (a) FTIR spectrum of PGD surfaces treated with different hydrolysis protocols. (b) The relative amount of -COOH groups of various hydrolyzed PGD, compared to the peak area difference between 0.1M and untreated PGD, in fold change.

The surface hydrophilicity of various PGD films was comparatively evaluated by a water contact angle measurement using a sessile drop method (**Figure 3.5 a**). The water contact angles determined on the hydrolyzed PGD surfaces ranged from approximate 0° to 60° (**Figure 3.5 c**). The untreated and 0.1M-5 PGD film were the most hydrophobic, while 0.1M-60, 0.5M-30, 0.5M-60, and 1M-15 groups were super-hydrophilic with nearly zero water contact angle. The surface hydrophilicity of the PGD surfaces was enhanced after the alkaline hydrolysis, especially when used 0.5 M NaOH or more than 30 min for hydrolysis treatment. Increasing hydrolysis treatment level, both in adding treating time and increasing treating dose, typically enhanced PGD surface hydrophilicity. However, there was a rise in water contact angle and a decrease in hydrophilicity on 1M treated samples while the treatment time is higher than 15 min, which may be caused by the change of surface morphology. This could be supported by the evidence of abundant mass loss presenting in 1M NaOH-treated groups (**Figure 3.5 b**). There was no effect of bulk degradation in 0.1M NaOH groups. Treatment condition in 0.5M NaOH caused mass loss of PGD until reached 30 min hydrolysis time. According to the surface charge profile of each hydrolyzed sample, we found the increase of hydrophilicity during hydrolysis treatment came along with the increase of the exposure of -COOH and -OH functional groups, only when its weight loss is not bigger than 5%.

The surface morphology and roughness of both untreated and alkaline-treated PGD scaffolds were simultaneously examined by scanning electron microscope (SEM) and atomic force microscopy (AFM), respectively. According to SEM images, we found the hydrolysis treatment level altered the surface topography and roughness of PGD (**Figure 3.6**). PGD without hydrolysis was a little rough with the presentation of a large number of spikes and micro-hillocks on the surface (**Figure 3.6 a**). It was noted that both hydrolysis reaction time and concentration impacted the surface morphology and roughness of the hydrolyzed PGD, especially when 1M NaOH was used. Treated in 0.1M NaOH gradually reduced the number

and size of spikes on PGD surfaces. When treated in 0.5M NaOH, increasing hydrolysis time at first decreased the surface spikes of PGD, but then remarkably increased the size of spikes as treated above 30 min. While in 1M NaOH, the PGD surface started to degrade thus generating micro-scale vales (10-20 μm width). Among all hydrolyzed PGD, 0.5M-30, 0.5M-60, 1M-15, and 1M-30 samples possessed the most etched surface with the largest pits throughout the surface, compared with other treatment conditions. Overall, NaOH treatment in 0.1M concentration reduced the size of hillocks, decreased surface roughness, and led to a smooth surface, while high hydrolysis level led to abundant erosion of the surface, raised roughness, and formation of micro-scale vales on the length-scale of chondrocytes.

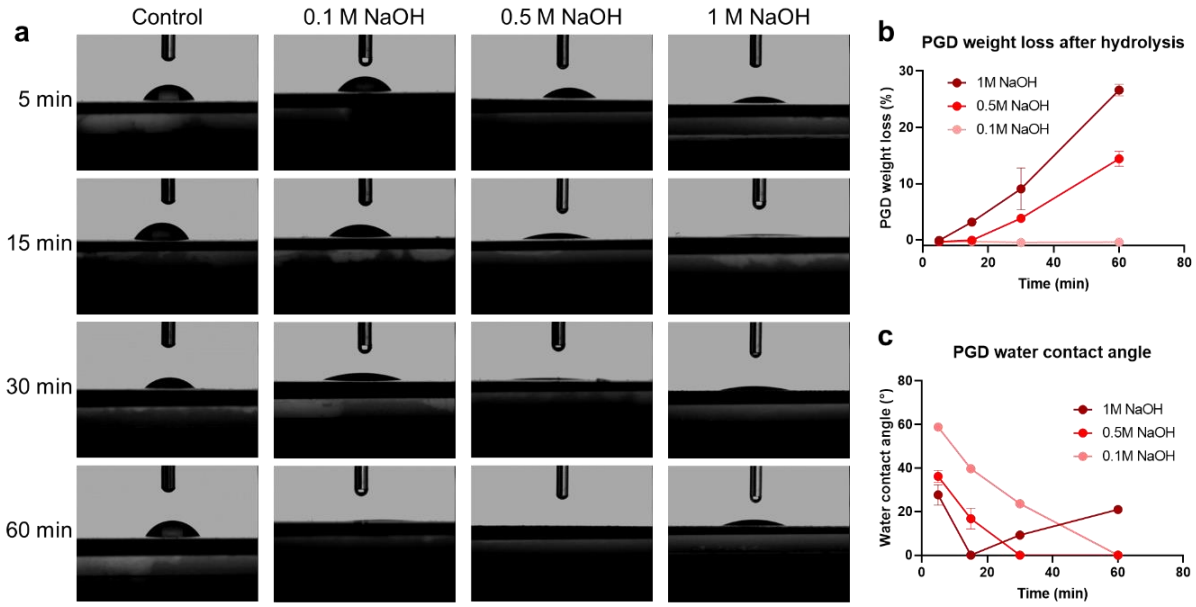

Figure 3.5 Hydrolysis level enhanced the surface hydrophilicity of PGD (a) & (c) Water contact angles of PGD surface that treated by different hydrolysis profiles. Data represented as mean ± s.e.m. (b) Total mass loss of PGD film due to degradation by different levels of hydrolysis. Data represented as mean ± s.e.m.

Alterations in the topological profile and roughness of hydrolyzed PGD surfaces were further investigated by AFM (**Figure 3.6 b**). A higher average surface roughness (Ra) means a rougher surface. Compared to untreated PGD, hydrolyzed PGD treated in 0.1M NaOH had reduced Ra, smooth surface, and no spikes but only swallow pits at a cellular length-scale (30 μm × 30 μm).

While using the 0.5M-15 condition, the size of pits and spikes on hydrolyzed PGD greatly increased. These AFM results were in accordance with the SEM results shown above.

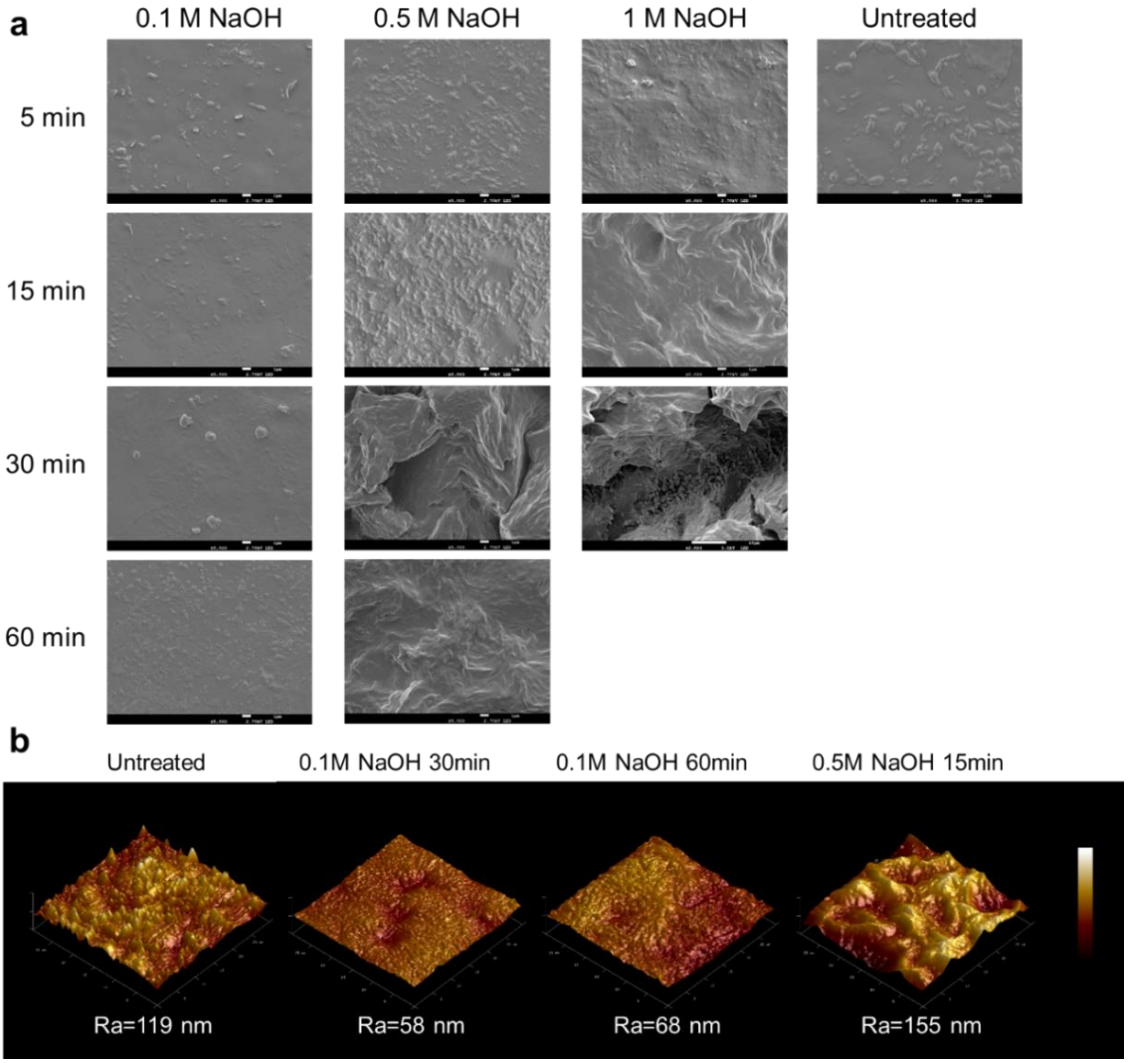

Figure 3.6 Hydrolysis level altered the surface topography of PGD (a) SEM surface topography of various PGD films, 1000X, Scale bar: 1 μm. (b) AFM micrographs of surfaces of various PGD scaffolds (at 30 μm × 30 μm area), Ra: average surface roughness.

3.4.2.2 Combinatorial Effect of Surface Charge and Roughness on Chondrocyte Shape

Immunofluorescent staining of F-actin and focal adhesion protein staining was conducted to evaluate the influence of hydrolysis intensity on cell shape. HACs attached and proliferated on hydrolyzed PGD films, indicating their cytocompatibility (**Figure 3.7**).

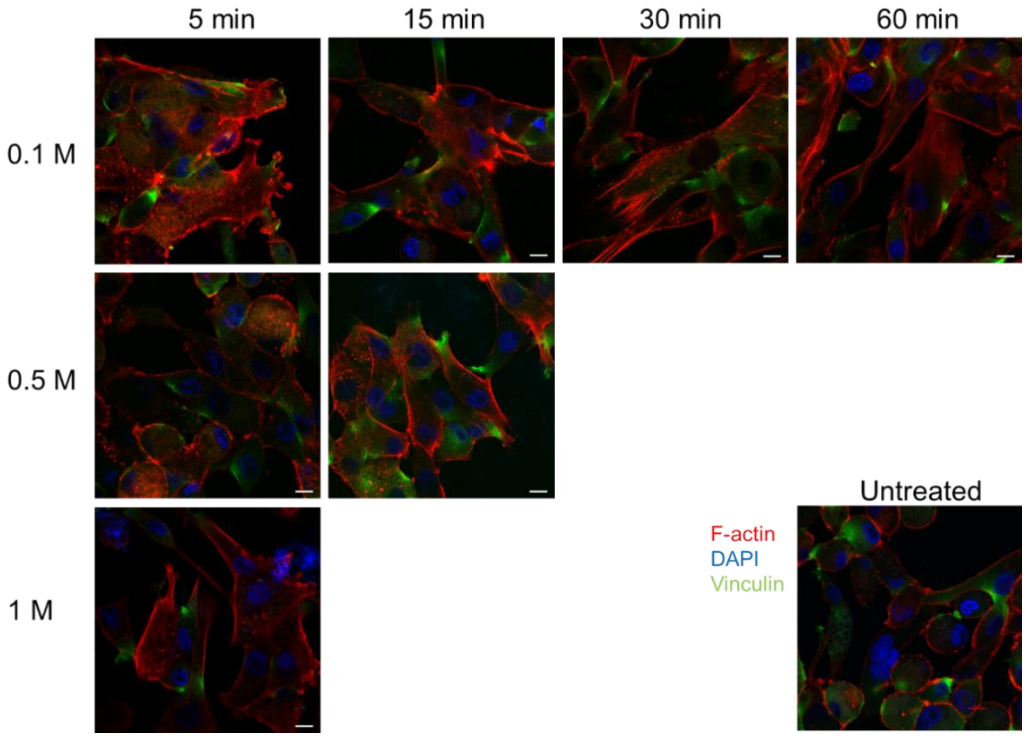

Figure 3.7 Hydrolysis level influenced chondrocyte shape on PGD. (a) Fluorescence images of phalloidin TRITC staining (F-actin, red), DAPI staining (nucleus, blue), and vinculin staining (focal adhesion protein, Green) on chondrocytes-seeded PGD films with various hydrolysis conditions. Scale bar: 10 μm.

The cell morphology was altered by the hydrolysis condition on day 2 culture. Vinculin is a cytoskeletal protein associated with focal adhesion and adherent junctions, which function in adhesion and/or signaling between the extracellular environment and the cell [79]. HACs on untreated PGD had a round cell shape, representing a chondrogenic phenotype. HACs on PGD treated in 0.1M NaOH and 1M NaOH condition showed stretched polygonal shape, while the hACs on 0.5M samples successfully retained the round cell shape (**Figure 3.7**). Increasing treatment time in 0.1M NaOH led to a higher single-cell area and a more stretched hAC morphology. While treated with alkaline in 5 min, increasing alkaline concentration first led to round morphology of hAC (0.5 M group), and then led to a stretched shape of hAC (1 M group). The 0.1M-60 and 1M-5 groups showed the most stretch cell shape and reduced amount of vinculin staining compared to the uncoated group, suggesting potential changes in the phenotype of the chondrocytes. With a similar surface charge, PGD treated with 0.1M-30 and

0.5M-5 conditions induced greatly different cell shapes (**Figure 3.4 b & 3.7**). Considering the difference in surface topography between PGD treated by 0.1M-30 and 0.5M-5 (**Figure 3.5 a**), surface topography played a role in guiding cell shape on PGD. These results implied that the moderate surface roughness and hydrophilicity improved by the hydrolysis treatment supported cell attachment.

3.4.2.3 Combinatorial Effect of Surface Charge and Roughness on ECM Production

The results of sGAG production indicated the combinatorial effect of surface chemistry, e.g., hydrophilicity and charge density, and physical parameters, e.g., topography and roughness, on chondrocyte ECM production on PGD (**Figure 3.8**). The TCP and untreated PGD induced less sGAG accumulation and looser aggrecan aggregation than treated PGD samples, especially 0.5M-5 and 0.5M-15. The hydrolysis condition in 0.1M NaOH gradually enhanced the PGD surface hydrophilicity (**Figure 3.5 c**) and surface charge (**Figure 3.4 b**) by adding treatment time, however, increasing treatment time did not change the cell shape (**Figure 3.6**) and sGAG/DNA production (**Figure 3.8 a**), probably due to a slight difference of surface topography among those samples (**Figure 3.7**). Enhanced surface charge by prolonged treatment period in the 0.1M NaOH group resulted in higher total sGAG production, which was consistent with Alcian blue staining results, while the 0.1M-30 group showed denser and more homogeneous distribution of sGAGs than the 0.1M-5 and 0.1M-15 groups (**Figure 3.8 b**).

The slightly rough surface of hydrolyzed PGD (0.5M-5, 0.5M-15, and 1M-5) could stimulate sGAG synthesis more effectively than a smooth surface (0.1M NaOH treated PGD), according to higher sGAG/DNA production (**Figure 3.8 a**) and more robust ECM accumulation (**Figure**

3.8 b). hACs with a round shape that grew on PGD treated by 0.5M-5 and 0.5M-15 resulted in enhanced ECM accumulation compared to other flatten-shaped cells. Moreover, with similar surface charge density (**Figure 3.4 b**) but different cell shapes (**Figure 3.6**), PGD treated by 0.5M-5 condition produced significantly higher sGAG content per DNA than 0.1M-30 condition, while the total sGAG production and Alcian blue staining results of those two groups were similar.

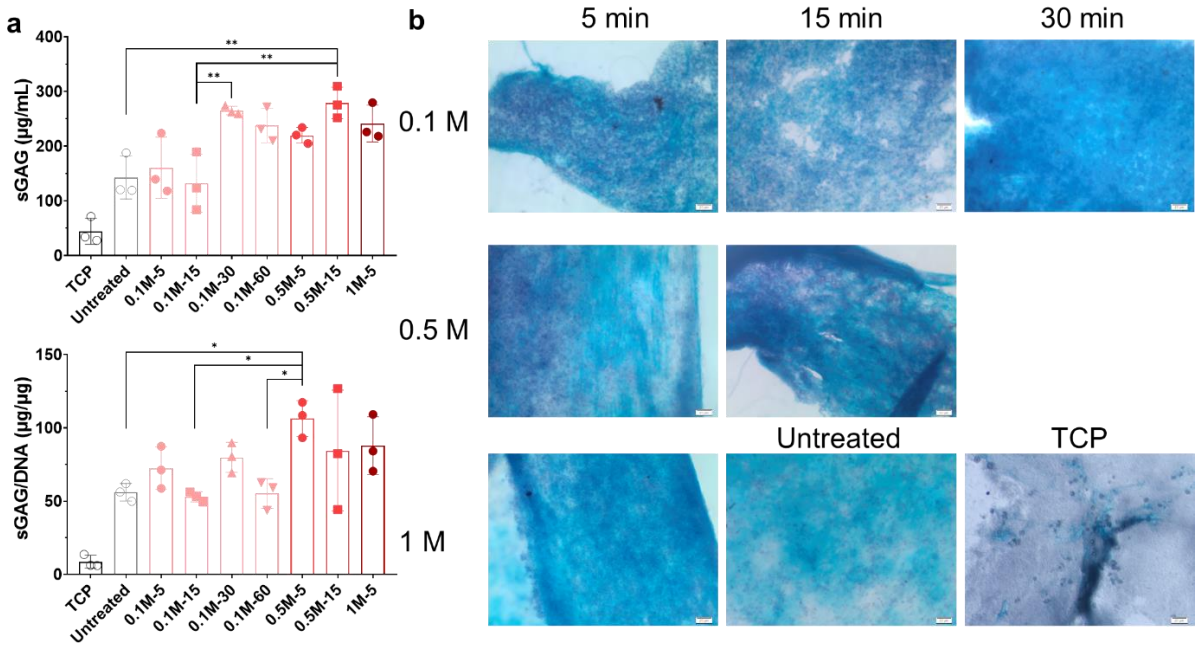

Figure 3.8 Surface charge and roughness co-modulated ECM production on PGD films. (a) sGAG production of hACs on PGD films treated with different hydrolysis conditions after 28-day culture. sGAG production was measured by DMMB assay and normalized to DNA contents. TCP: tissue culture plate. Data represented as mean ± s.e.m. Significant difference is indicated by * $p<0.05$, ** $p<0.01$, by one-way ANOVA corrected with Tukey's multiple comparison method. (b) Alcian blue staining for the distribution of accumulated aggrecan after 28-day culture. Scale bar: 20 µm.

These results revealed a combinatorial effect of multiple surface parameters on the ECM-anabolic activity of hAC. Overall, PGD films that were treated with alkaline conditions of 0.5M-5 and 0.5M-15 developed with the round cell shape (**Figure 3.7**) and highest sGAG content (**Figure 3.8 a**), while all the treated groups generated robust ECM compared to TCP (**Figure 3.8 b**).

3.5 Discussion

Prolonged monolayer expansion of chondrocytes is a necessary process in clinical treatment of large cartilage defects during an autologous chondrocyte implantation procedure. The phenotype of chondrocytes may change dramatically when cultured for a long period on a tissue culture plate [29]. In this circumstance, the gene expression of chondrocytes shifts from a differentiated phenotype to another resembling that of fibroblasts, which causes the production of type I procollagen, fibronectin, and small noncartilaginous proteoglycans [29]. With this change in cell phenotype, the chondrocyte morphology changes from round to flat. In the end, the quality of the matrix synthesized by the chondrocytes deteriorates significantly from that of normal cartilage. In this work, we aimed to enhance the ability of hAC to synthesize robust ECM by developing a cell-favorable surface environment to enhance hAC redifferentiation using (1) ligand coating and (2) surface hydrolysis.

In Aim 1a, we found that coating cartilage ECM ligands onto PGD 2D surfaces significantly facilitated the formation of a round cell shape and the production of sGAG. The large pores of the porous synthetic scaffold usually provide a 2D environment for cell attachment due to a much larger magnitude of pore size compared to single cell size and 2D culture on stiff substrates (like tissue culture plate, TCP) leads to aberrant chondrocyte phenotypes and loss of the differentiated phenotype. Our results revealed that introducing ECM ligands in scaffold can help to maintain round chondrocyte morphology and its differentiated phenotype. This could be supported by the cell-ligand binding complex. The binding of surface receptors to ligands is the molecular basis of the initial adhesion of transplanted chondrocytes to surrounding cartilage in the defect site [80]. After initial attachment, integrins on the chondrocytes then will be involved in proliferation, survival, differentiation, matrix remodeling, and response to mechanical stimuli [81]. To be specific, chondrocytes express integrin receptors, for example,

α1β1 and α10, has a function in binding to collagen ligands. Studies have shown that even with a high population doubling number, chondrocytes on the pure collagen type I substrate were round-shaped and produced collagen type II, whereas the on the TCP substrate chondrocytes lost their differentiated phenotype [51]. However, our results showed hAC cultured on collagen type I coated PGD grew into a flattened, stretched shape (**Figure 3.2 a**). This was possibly caused by the higher stiffness of PGD than Col I substrate and it has been shown that stiff matrices tend to induce a flattened morphology of chondrocytes [32]. Conversely, our results showed that hyaluronic acid coating of PGD successfully induced a round hAC morphology and higher synthesis of sGAGs compared to uncoated and other ligand-coated surfaces. This may be explained by previous studies which showed that cell binding to hyaluronic acid, via surface receptors including CD44 and RHAMM, triggers a sophisticated signaling pathway causing chondrocytes to maintain their natural phenotype [82]. Therefore, our results suggested using hyaluronic acid in the coating is a better way to improve the chondrogenic ability of scaffolds in cartilage tissue engineering.

The study has shown the surface hydrolysis of ester bonds, which exposes carboxylic acid and alcohol groups, can improve integrin binding, thus improving the ability of cells to adhere to the surface of poly(ε-caprolactone) scaffolds [78]. Our results support this outcome, demonstrating that the improved surface properties, e.g., hydrophilicity and moderate roughness, facilitated a round chondrocyte shape (day 2) and enhanced subsequent ECM production (day 28). Interestingly, our results indicated altering one surface parameter alone did not optimally facilitate chondrocyte redifferentiation on a biomaterial platform. We found a combinatorial effect of surface charge density and roughness on cell shape and ECM production, accomplished by comparing the cell behavior on PGD under various hydrolysis conditions.

Controlling hydrolysis conditions can simulate and regulate the hydrophilicity, wettability, and amount of exposed functional groups of PGD surface, which can be linked to the improvement of physical coating efficiency or chemical immobilization potential of the biomaterial. Good wetting is generally related to good adhesion of coating solutions. The carboxylic acid group is a versatile functional group for multiple ways of chemical reactions.

We found that the slightly rough surface of hydrolyzed PGD (0.5M-5, 0.5M-15, and 1M-5) could stimulate sGAG synthesis more effectively than a smooth surface (0.1M NaOH-treated PGD). Though these rough surfaces differently induced cell shapes in the early culture period, there was no significant difference between the sGAG production and aggrecan distribution of these samples, indicating that cell shape is not the only factor that could guide cell fate. The scaffold parameters such as surface charge and topography influenced cell shape in the short-term but may not continuously impact cell function. This could be due to an increase in cell-ECM interactions that occur outside of the initial scaffold properties as the neo-cartilage forms. Another potential factor is other microenvironmental cues not examined in this analysis that may have a more long-lasting impact on cell function than the initial surface properties. Despite that, this work provided sufficient evidence that surface charge and surface topography work together to modulate cell behavior on PGD *in vitro* culture.

3.6 Conclusion

In Aim 1a, we found there is a combinatorial effect of surface ligand density and composition on chondrocyte shape and ECM production. The morphology of hACs on PGD in short-term culture is regulated by the type of ligand coating. sGAG production of hACs on PGD in long-term culture is regulated by not only the ligand retention level but also the type or combination

of ligand coating. Overall, the ligand coating parameters that could influence chondrocyte behavior include a) component of coating, b) mass or density of ligand, and c) method of coating, suggesting a potential guideline for optimizing micro-environmental cues for cartilage regeneration in 3D scaffolds. In Aim 1b, we found there is a combinatorial effect of surface charge density and roughness on cell shape and ECM production. The chemical composition, surface roughness, and wettability of PGD were drastically altered by the alkaline hydrolysis, and those surface parameters worked together to guide cell behavior. Our results demonstrated that moderate roughness and enhanced hydrophilicity of PGD surfaces provided a favorable environment for the chondrocytes ECM production without changing the bulk properties. Therefore, surface hydrolysis of PGD is a viable strategy to increase its hydrophilicity and improve cell function.

Chapter 4

Develop Porous PGD Scaffolds and Investigate the Effect of Pore Geometries on Cellular Level Strains that Developed inside 3D Scaffolds

4.1 Abstract

Synthetic polymeric scaffolds play an important role in establishing the microenvironment for chondrocytes in engineered cartilage. A porous three-dimensional (3D) structure and interconnected pore network allow nutrient and waste exchange, which supports extracellular matrix (ECM) production of the chondrocytes. Additional scaffold design parameters, such as ligand coatings and biomechanical properties, also affect the quantity and quality of neo-cartilage tissue produced in regenerative strategies by mediating cell attachment and establishing the local strain environment. Poly(glycerol-dodecanedioate) (PGD) is a novel biodegradable elastomer that has nonlinear elastic mechanical properties similar to native cartilage, making it a viable scaffold choice for cartilage tissue engineering applications. However, harsh curing environments (high temperature and vacuum) limit the feasibility of common strategies of pore creation without significant loss of scaffold stiffness. Here we have developed porous PGD (pPGD) scaffolds with tailorable, interconnected pore structures using an inverse molding method and evaluated the range of scaffold structural parameters achievable (pore size and porosity) and subsequent mechanical properties. Finally, we used finite element analysis to determine if the local strain fields that developed inside the pores under load could be tuned to be within the range shown to have an anabolic effect on chondrocyte function. Porous PGD scaffolds were created with pore sizes ranging from 250 – 1000 μm, resulting in

20 – 50% porosity. The tensile strains that develop along 31% – 71% pore surfaces inside of pPGD scaffolds, according to varying pore size and porosity, were at levels shown to stimulate chondrocyte ECM production. Porous PGD scaffolds with lower porosity and smaller pore size had a higher percentage of beneficial strain, suggesting that the pore structural parameters could be tuned to optimize cellular-level strain profiles. These results suggest that pPGD scaffolds have the potential to guide cartilage regeneration.

4.2 Introduction

Articular cartilage has a limited ability to self-repair, which often causes traumatic injuries to progress into post-traumatic osteoarthritis (PTOA) [83]. Chondrocyte-based tissue engineering is an appealing approach for treating cartilage defects and preventing the onset of PTOA [84]. Among the biomaterials being investigated for cartilage tissue engineering, polymers are one of the most flourishing areas since they are easily processed into porous scaffolds that sustain cell proliferation and can be tailored for desired mechanical properties and degradation profiles [85]. An ideal polymer scaffold for articular cartilage regeneration should provide the following characteristics [86]: (i) a 3D interconnected porous structure to allow cell attachment, proliferation, differentiation, and extracellular matrix (ECM) production and promote nutrient and waste exchange, (ii) a biocompatible and bioresorbable substrate with controllable degradation rates, and (iii) mechanical properties similar to natural cartilage tissue to withstand the surrounding harsh biomechanical environment.

Polymeric scaffolds have the potential to support chondrocyte function while protecting them from the load. By incorporating strategies and techniques for creating, controlling, and characterizing scaffold architecture and cell-material interactions into the scaffold design

process, the local environment can be tuned to enhance cell function. Modulations of scaffold parameters, such as pore size, total porosity, material surface chemistry, and biomechanical properties, have been shown to enhance cartilage tissue regeneration during *in vitro* co-culture [4]. Optimization of scaffold design via manipulating these scaffold parameters to create functional cartilage normally starts with *in vitro* models and computational models. The influence of these parameters on chondrocyte function has previously been demonstrated in citrate-based scaffolds [87, 88]. Studies show proper pore size and porosity of a scaffold support the maintenance of the chondrocyte phenotype and promote the biosynthesis of cartilage-related ECM components [15, 49, 50]. These parameters not only determine the macroscale properties of neo-cartilage, which must facilitate joint function, but they also affect the mechanotransduction in chondrocytes by altering the local environmental strain fields around the cells [89]. An optimal scaffold will conduct anabolic mechanical signals to the cells while protecting them from physiologic joint loads.

Cells can sense the external mechanical and ligand cues and translate those cues into intracellular signaling, which influences cell behavior. There are many cellular structures and pathways involved in mechanical sensing and transduction into changes in gene expression and protein production. These include structural elements, such as stress fibers, focal adhesions, and integrins, activating mechanotransduction pathways such as RhoA/ROCK and Yap/Taz [89]. Binding to ECM ligands induces mechanical sensing through actin fibers and activation of integrins, cell subsequently adjusts its cell-ECM interaction strength and finally alters its shape, proliferation, migration, and phenotype through multiple pathways[89]. The scaffold design process hence requires the optimal structural parameters and ligand coating for the desired level of mechanotransduction since chondrocytes reorganize the ECM components of articular cartilage in response to the external load [72]. Previous work has shown that, in monolayer culture, loading between 3–10% cyclic tensile strain, 0.17–0.5 Hz, and 2–12 h led

to anabolic responses of chondrocytes, and beyond that range caused catabolic events to predominate [72]. Due to the 2D nature of cell morphology when they attach to porous scaffold surfaces, this important design parameter should be incorporated into the design of polymer scaffolds.

Herein we report the design and characterization of porous scaffolds created from poly(glycerol-dodecanedioate) (PGD) for cartilage tissue engineering. PGD is a novel biodegradable elastomer formed by polycondensation of glycerol and dodecanedioic acid[46]. It was first reported in 2010 for potential use in soft tissue engineering applications because of its elastomeric mechanical properties, low *in vitro* degradation rate, shape memory behavior, and good biocompatibility[46, 47, 74]. PGD has nonlinear elastic properties at body temperature and elastic-plastic behavior at room temperature[46, 47]. Moreover, the mechanical properties of PGD can be controlled by varying the curing time and temperature, resulting in materials with a range of moduli comparable to soft tissues, e.g., cartilage [47]. Those properties make PGD a viable model choice for scaffold optimization in cartilage tissue engineering. However, the application of PGD for cartilage tissue engineering is hindered by the harsh curing conditions (high temperature and vacuum), which limits the number of strategies that can be used to create a porous structure while maintaining the stiffness of the scaffold. Here, an inverse molding method was used to create porous PGD (pPGD) scaffolds with tailorable, interconnected pore structures. The range of scaffold structural parameters achievable (pore size and porosity) were evaluated with microcomputed tomography (micro-CT), and their mechanical properties were evaluated via compressive testing. The effects of ligand coating on the morphology, metabolic activity, and ECM synthesis of human articular chondrocytes (hACs) were also evaluated. Finally, the effect of porosity and pore size on the local strain fields inside simulated pPGD scaffolds was evaluated using finite element analysis.

4.3 Methods

4.3.1 Porous PGD Fabrication

Prepolymer and curing:

PGD prepolymer was synthesized and then cured following methods described by Solorio et al[47]. Briefly, PGD pre-polymer was synthesized by mixing glycerol and dodecanedioic acid with a 1:1 molar ratio at a 120 °C flask under nitrogen and stirring conditions for 24 h. The viscous pre-polymer was then cast into silicone molds and transferred into a vacuum oven at 130 °C for 48 h. A vacuum was pulled and maintained at 90 mTorrs for the duration of the curing process, to get the solid nonporous PGD blocks.

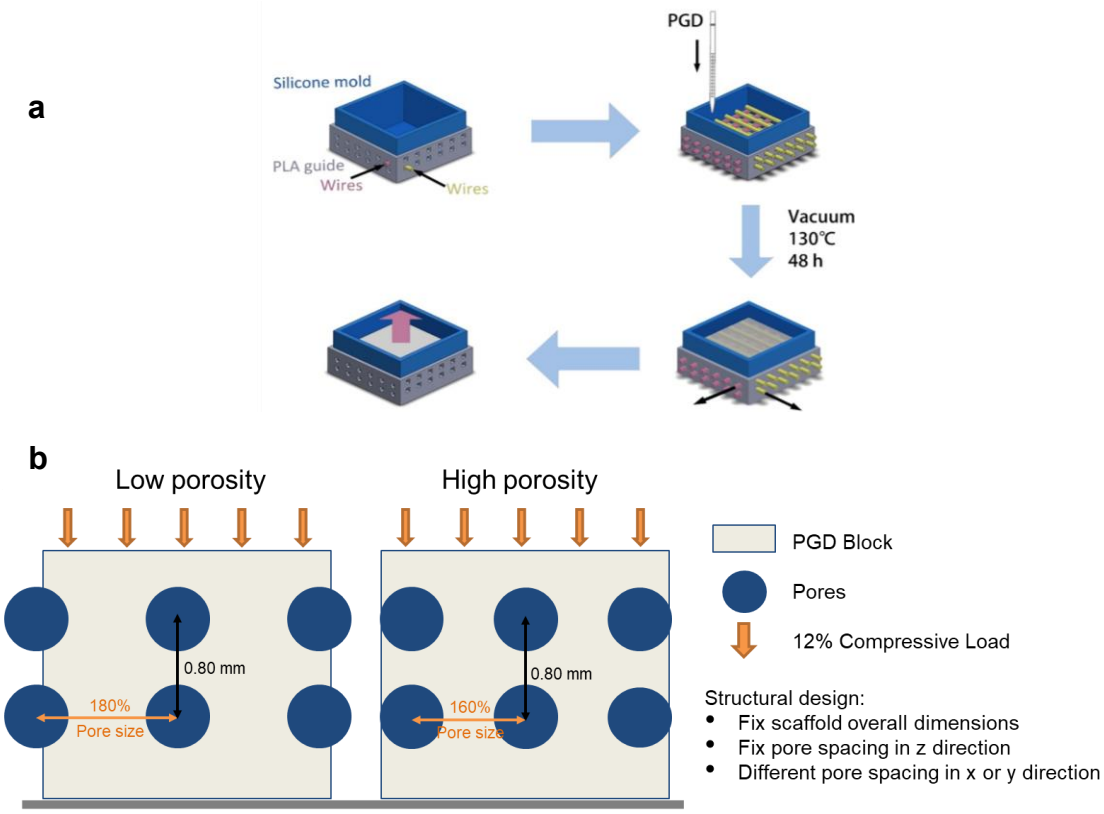

Figure 4.1 Experimental designs of pPGD scaffold fabrication and finite element models. (a) Schematics of pPGD scaffold fabrication via inverse molding. The position of the wires was precisely located by polylactic acid guides (grey). The silicone mold (blue) and Teflon-coated stainless-steel wires (yellow and pink) are shown. Wires were organized layer-by-layer in the two directions (the angle between the two directions is 90 degrees). (b) Schematics of geometrical design for simulated pPGD scaffolds. The porosity of the simulated pPGD scaffold was altered by changing the pore spacing horizontally.

Porous Scaffold fabrication

The pore size of pPGD scaffold was controlled using Teflon-coated stainless-steel wires as outlined in **Figure 4.1 a**. Due to its chemical inertness and thermostability, Teflon-coated wires were easily removed after PGD curing and therefore presented a good choice for creating voids in the thermoset PGD scaffolds. PGD prepolymer was synthesized as described above. To control the wire position, polylactic acid (PLA) guides were designed in SOLIDWORKS and then printed on a 3D printer (FlashForge 3D Printer Creator Pro). The PLA guide was placed into a silicone mold and Teflon-coated stainless steel wires (McMaster-Carr) 250 μm, 500 μm, 750 μm, or 1000 μm in diameter were pierced through the wall of the silicone mold, and their final position was controlled by the PLA guide (**Figure 4.1 a**). Porosity was controlled by decreasing the spacing between wires, thereby increasing the wire density. The PGD prepolymer was then cast into the mold and cured under a 90 mTorr vacuum maintained at 130°C, for 48 h. After curing, the wires were removed and the pPGD scaffolds were peeled out of the silicon mold. Each pPGD scaffold was then cut into cylinders 6 mm in diameter and 3 mm in height.

4.3.2 Scaffold Structural Parameters Analysis

The scaffold micro-geometry was reconstructed from microcomputed tomographic (μCT) images acquired using Scanco μCT 100 system. Samples (N=4) were scanned, using a 4 μm resolution and a pixel size of 4 μm. The 3D models of the scaffold geometry were reconstructed from the μCT images using Materialise Mimics and the scaffold volume and total volume were quantified throughout the sample geometry. The porosity was calculated using the following equation after quantifying the scaffold volume.

$$Porosity = 1 - \frac{V_{porous}}{V_{total}} \times 100\%$$

Where V_{porous} is the volume of the porous structure and V_{total} is the total volume of the enclosed structure.

4.3.3 Mechanical Testing

To analyze the pore parameter effects on the mechanical properties of pPGD scaffolds, compression testing was conducted at 37 °C. MATLAB (The MathWorks Inc., MA) software was used to fit a one-term Ogden model to experimental data to obtain the shear modulus of each pPGD scaffold. Compressive testing was conducted on 6 mm pPGD cylinders within a custom-built temperature control chamber using an MTS system equipped with a 500 N load cell and a metal platen. Samples (N = 4) were tested in the chamber maintained at body temperature (37°C). Compression was applied at a rate of 2 mm/min, and samples were compressed to about 60% strain at 37 °C. The mechanical test data obtained at 37°C was then fit to a one-term Ogden constitutive model for nonlinear hyperelastic materials using custom MATLAB algorithms. In brief, the one-term Ogden model was based on a strain energy function of the form:

$$W\left(\lambda_1, \lambda_2, \lambda_3\right) = \frac{\mu_1}{2}\left(\lambda_1^{\alpha_1} + \lambda_2^{\alpha_2} + \lambda_3^{\alpha_3} - 3\right)$$

Where W was the strain energy function, λ_i denoted the stretch ratios in the x_1, x_2, and x_3 directions, and μ_1 and α_1 were constants that were fit to the experimental data. For the uniaxial compression test in this study, assuming the specimen was tested in the x_3 direction, the resulting normal 1st Piola-Kirchoff stress was calculated as

$$T_3 = \frac{\mu_1}{\lambda_3}(\lambda_3{}^{\alpha_1} - \lambda_3{}^{\frac{\alpha_1}{2}})$$

The normal stress was calculated from the experimental compressive test by dividing the applied force by the initial specimen area. The coefficients from the model (μ_1 and α_1) then were fitted to the experimental stress using the *fmincon* routine in the MATLAB optimization toolbox. The results were further constrained using the Baker-Eriksen inequality [47]

$$(\lambda_3 \frac{\partial w}{\partial \lambda_3} - \lambda_2 \frac{\partial w}{\partial \lambda_2})(\lambda_3 - \lambda_2) > 0$$

The coefficient of determination (R^2) was calculated for fitting quality, and the estimated shear modulus (μ) of the specimen was calculated by

$$\mu = \mu_1 \alpha_1 / 2$$

4.3.4 Finite Element Analysis

To determine how pore size and porosity affect the strains that develop within the pores of pPGD scaffolds during loading, finite element analysis (FEA) was performed on the simulated geometries of pPGD scaffolds using COMSOL. The simulated pPGD geometries were modeled as 3mm cubes with pore sizes of 250 μm, 500 μm, 750 μm, or 1000 μm. To vary the porosity of the model, the distance between the centers of each pore was fixed to 160% pore size for high porosity groups or 180% pore size for low porosity groups (**Figure 4.1 c**). All models were meshed with a tetrahedral volume element with a similar mesh size (minimum mesh size = 0.055 mm). The one-term Ogden constants of nonporous PGD that were obtained from mechanical tests and hyperelastic fitting as described above were applied to the scaffold

mesh elements. The lower surface of the model was constrained in all directions and a 12% prescribed displacement (0.3 mm) in the z-direction was applied on the upper surface. This boundary condition was chosen to mimic the level of cartilage deformation in the knee joint during 30 min of standing, according to the highest mean strains (12%) over the femoral-tibial contact area [90]. The maximum first principal strain (maximum tensile strain) was calculated in the central pores of each simulation. The percentages of nodes on the central pore surface that denoted strain of 3 – 10 %, which has been shown to be beneficial for chondrocyte function [72], were calculated.

4.3.5 Statistical Analysis:

Unless indicated otherwise, results were analyzed using a one-way ANOVA and Tukey post-hoc test for multiple comparisons in GraphPad Prism 8.0 (GraphPad Software, San Diego, CA). The porosity, surface area, and shear modulus of pPGD scaffolds were compared across different pore size groups. The criterion for statistical significance was $P < 0.05$ in all tests.

4.4 Results

4.4.1 Geometry Parameters of Porous PGD Scaffolds Fabricated by Inverse Molding

The 3D reconstructions of the pPGD μCT images confirmed that the inverse molding approach successfully fabricated PGD scaffolds with the desired pore diameters, well-aligned pore structure, good interconnectivity (**Figure 4.2 a**). The porosity of pPGD scaffolds was successfully controlled by changing the diameter of wires. Increasing the pore diameter while maintaining the distance between each wire resulted in increased porosity (**Figure 4.2 b**). Pore

sizes of pPGD scaffolds achieved a range from 250 - 1000 µm, resulting in porosity in the range of 20 – 50%. The creation of a pore network inside bulk PGD significantly increased the surface area of constructs (**Figure 4.2 c**). Changing the pore size above 500 µm led to no significant change in the total surface area of the pPGD scaffold, while the 250 µm group showed a higher surface area than other porous groups.

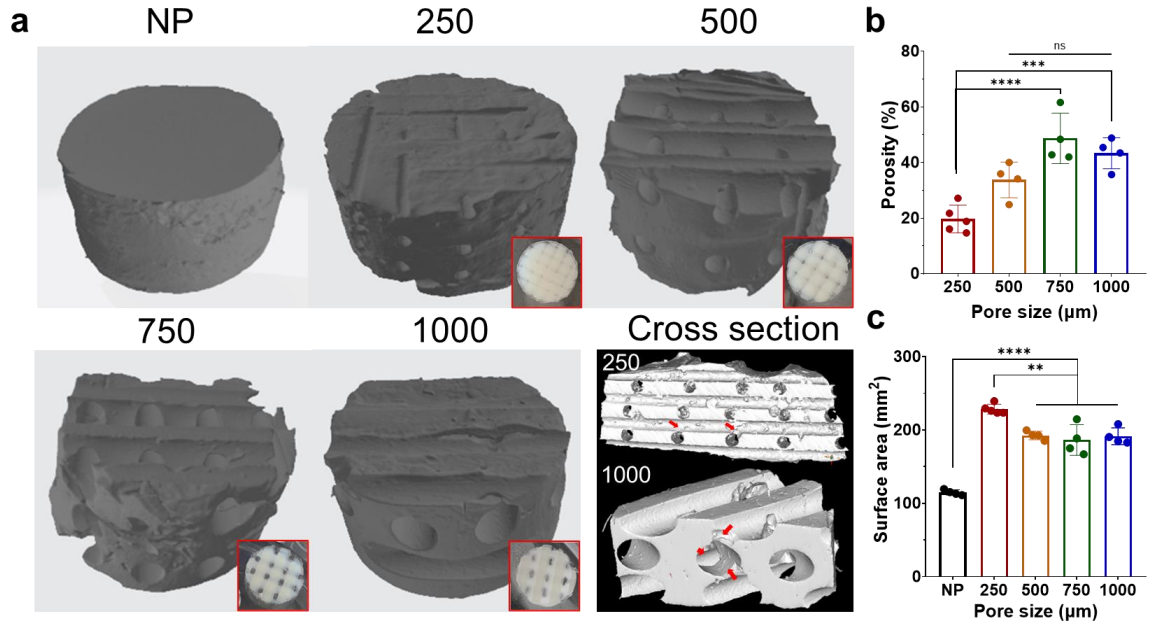

Figure 4.2 Geometries of porous PGD scaffolds. (a) 3D µCT image of nonporous PGD block and porous PGD scaffolds with varying pore diameters (250 µm, 500 µm, 750 µm, or 1000 µm). The red box at the bottom right corner: digital pictures of porous PGD scaffold (top view) immersed in 70% ethanol. NP: non-porous PGD scaffold. (b) Quantification of the porosity of pPGD scaffold with varying pore diameters. Data represented as mean ± s.e.m. Significant difference is indicated by *** $p<0.001$, **** $p<0.0001$ by one-way ANOVA corrected with Tukey's multiple comparison method. ns: no significance. (c) Quantification of the total surface area of pPGD scaffold with varying pore diameter. Data represented as mean ± s.e.m. Significant difference is indicated by ** $p<0.01$ and **** $p<0.0001$ by one-way ANOVA corrected with Tukey's multiple comparison method.

4.4.2 Geometry Parameters of Porous PGD Scaffolds Influenced Mechanical Properties

The stress-strain curve showed all groups of pPGD scaffolds and nonporous PGD bulk had nonlinear behaviors during compression (N=4, **Figure 4.3 a**). The R^2 value (> 0.95) indicated the good fittings of the one-term Ogden model to all the pPGD scaffolds (**Figure 4.3 a**). The pore structure had an influence on the maximum stretch ratio among all the scaffolds, indicating

the stiffness of pPGD scaffolds can be altered by changing the pore parameters. The scaffold with higher porosity had less stiff nonlinear elastic behavior (**Figure 4.2 a** & **Figure 4.3 a**). The shear modulus of the whole pPGD scaffold decreased with increasing porosity (**Figure 4.3 b**).

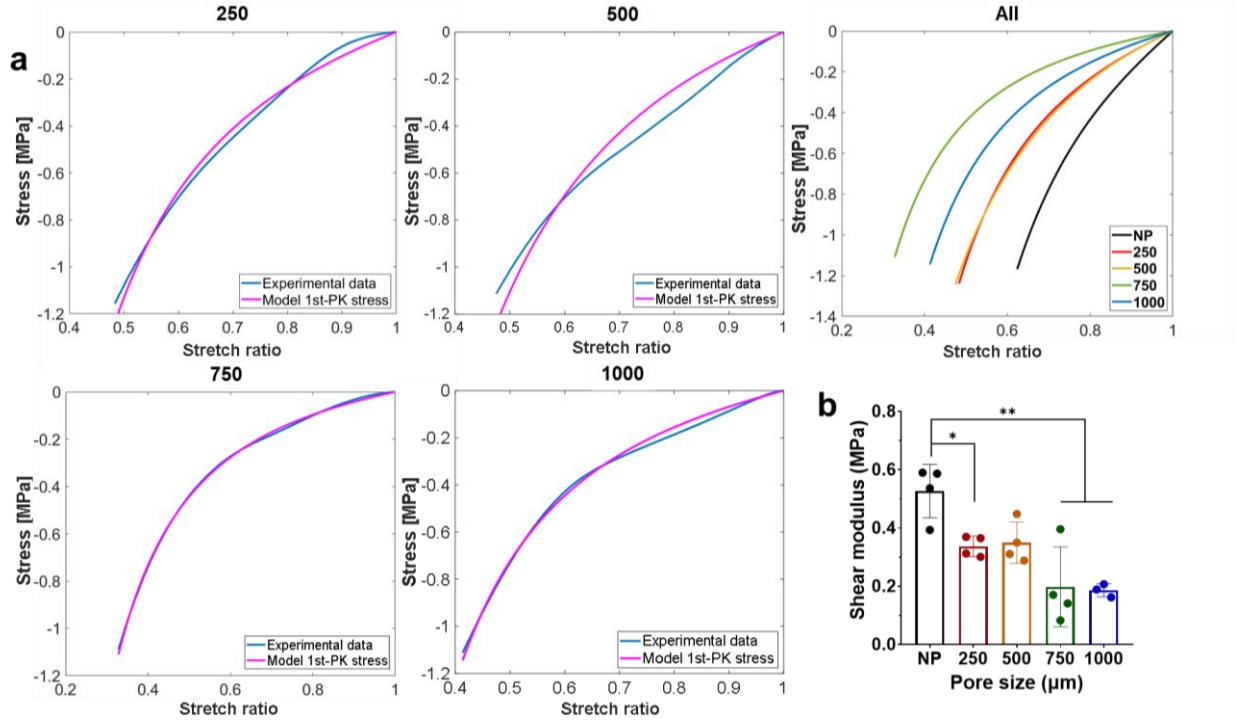

Figure 4.3 Pore size influenced the mechanical properties of pPGD scaffolds. (a) Stress-strain curve of pPGD scaffolds with varying pore sizes during compressive testing and corresponding one-term Ogden fitting curves. All: one-term Ogden fitting curves with all the pore size groups and nonporous PGD (NP). (b) Shear modulus of pPGD scaffolds with varying pore diameters. Data represented as mean ± s.e.m. Significant difference is indicated by * $p<0.05$ and ** $p<0.01$, by one-way ANOVA corrected with Tukey's multiple comparison method.

4.4.3 FE Modeling of Strain Fields inside Porous PGD Scaffolds

FEA was conducted to determine the influences of pore structure on cell-level strain inside pPGD scaffold. FEA analysis showed that the scaffolds with 1000 μm pore size had higher tensile strain than that of pPGD scaffolds with a smaller pore size (**Figure 4.4 a**). This was expected since the increasing pore size and porosity resulted in a decreased volume of the matrix and less stiffness. The strain fields inside the central pore best represented the strains

within the internal pores of the scaffolds and so these were focused on in FEA outcomes. All models showed that most of the central pore's surface area experienced low (0 – 10 %) strain. The minimum strain occurred on intersecting areas between the top and bottom pores, and the maximum strain occurred between each intersecting area. Therefore, the left and right sides of each central pore showed repeated patterns of the maximum and minimum area, while the top and bottom sides of each central pore showed more uniform strain distribution. The 1000 μm pore size group showed the maximum strain field (> 16 %) among all the groups on the intersecting area of the central pore (**Figure 4.4 a**). Scaffolds with higher porosity tended to have smaller stress concentration areas.

The overall tensile strain distribution inside the central pore of 250, 500, 750, and 1000 groups, ranged from 0 – 26 %, and the peak of strain distribution shifted to the right when the porosity decreased in all the pore size groups (**Figure 4.4 b**). Approximately 60% of nodes on the central pore of all groups, except 1000 groups, fell into the range of 3 – 10 %, which was shown as the range that induced anabolism in chondrocytes [72] (**Figure 4.4 b**). Despite the shift of the peaks between high and low porosity models, the porosity did not significantly alter the strain distribution pattern in the 250, 500, and 750 groups. The 1000 group is the only group that showed different strain distribution patterns between high and low porosity models. The 1000-H had two peaks within the beneficial strain range (3 – 10 %), while 1000-L showed one peak approaching higher strain (~ 12%). The percentage of the nodes in the central pore of each model that experienced the 3 – 10% beneficial strain, called %beneficial strain, was analyzed to better understand the strain distribution inside pores (**Figure 4.4 c**). The results confirmed that most of the nodes (> 60 %) fell in this specific strain range except in the 1000 groups. The %beneficial strain decreased slightly as pore size increased. The porosity had more influence on %beneficial strain than pore size, as scaffolds with lower porosity tended to have a higher percentage of beneficial strain, especially for the large pore size groups. The

highest %beneficial strain was shown in the groups with 500 μm pores.

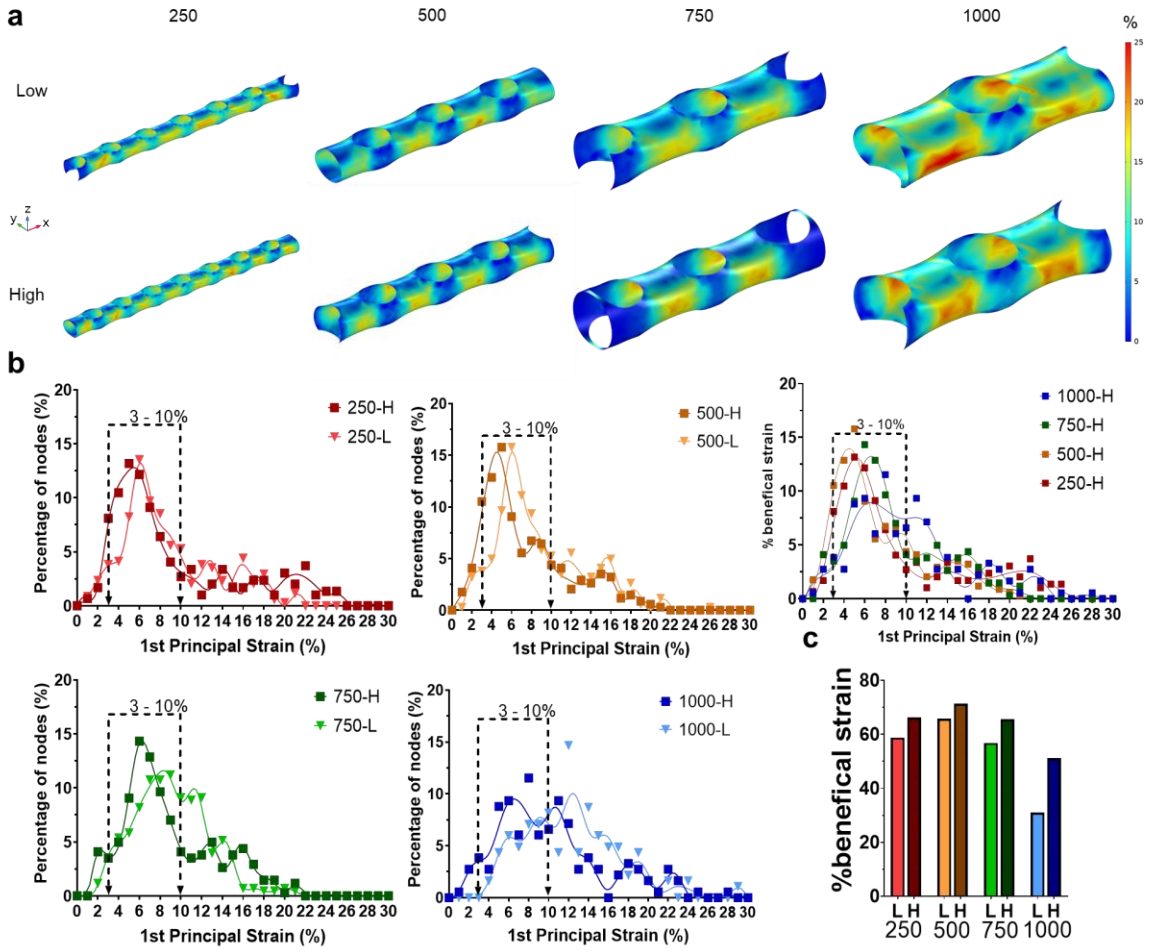

Figure 4.4 FE modeling of strain fields in pPGD scaffolds. (a) First principal strain fields of simulated pPGD models with 250 - 1000 μm pore size and two levels of porosities. (b) The distribution curve of 1st principal strain on the central pore of the pPGD models. L: low porosity, H: high porosity. y-axis: the percentage of nodes on the central pore that experienced a certain strain. Dotted line: the specific period of the distribution curve that shows the beneficial strain. (c) The percentage of nodes on the central pore that experienced the beneficial strain (3 – 10 %), also known as %beneficial strain.

4.5 Discussion

For cartilage tissue engineering applications, biomaterial scaffolds play a critical role in providing a 3D environment to support cell growth and matrix deposition while protecting the cells from joint loads. Successful scaffold design requires that several essential criteria be met — biocompatibility, biodegradability with a favorable resorption rate, suitable porosity and interconnectivity, and mechanical properties that can support tissue growth under native

mechanical loads. To develop and model a scaffold that satisfies these requirements, we selected an elastomer, poly (glycerol-dodecanedioate), which has been shown to be biocompatible, slow-degrading, and nonlinear elastic, with tailorable mechanical properties[46, 74], and thus has potential to support cartilage regeneration. To design porous PGD scaffolds to maximize ECM production, the influence of scaffold design parameters, such as pore structure and local strain field, was analyzed. We found changing the pore size and porosity of pPGD scaffold altered its surface area, shear modulus, and %beneficial strain that developed along the pore surface.

The importance of pore diameter and network organization in engineered cartilage tissue constructs is well-established. Common pore-creation strategies include solvent casting, particulate leaching, gas foaming, phase separation, fiber bonding, membrane lamination, melt molding, and freeze drying[91]. Solvent casting and particulate leaching techniques were developed to better control porosity and pore size [92-95]. However, the possible strategy for creating porous structures inside a thermoset polymer scaffold is limited by its harsh curing conditions, like high temperature, which precludes the use of particulate leaching methods using water-soluble agents that can create uniform pore structures such as sodium alginate agent. The salt particle leaching method is limited by lower hydrophilicity, lower achievable range of thickness (< 2 mm), and small pore size (< 250 um) of the scaffold. Laser microablation [96] and inversely solid freeform fabricated hydroxyapatite mold [48] were successfully conducted on poly (glycerol sebacate) (PGS), a thermoset polymer that has very similar polymerization and crosslinking conditions to PGD, to create uniform internal pores. However, those strategies still have limitations. The thickness of articular cartilage in a normal human adult knee is roughly 1.5–3 mm. Laser microablation is constrained by the number of layers (< two) and thickness (< 1mm) of the porous thermoset scaffold. Inversely solid freeform fabricated hydroxyapatite (HA) mold is a good way to design a customized geometry for

thermoset polymer, but it is a complex three-step process. Other methods, such as freezing dry, involved additional materials to achieve pore creation, which altered the native properties of PGS[97]. Our two-step inverse molding method can avoid the limitations in achievable sample thickness and in complex pore-creation processes.

The dimension, volume, and organization of 3D porous structures in PGD can be controlled by our inverse molding method. However, the layer-by-layer organization of the wires limited the possible pore structures that could be achieved with this method. For example, the minimum pore size achievable with this method was 250 μm due to the limited resolution of the 3D printed guide and unstable control of wire arrangement. However, previous studies show that pores < 300 μm in diameter induced chondrocytes to chondrogenic differentiation, while larger pore size induced osteogenic differentiation *in vitro* [50]. Other studies show that larger pores (400 – 1000 μm) can improve cell proliferation and cartilage-like matrix deposition [49, 98]. The disparities in these conclusions may be caused by the variety of material properties, scaffold manufacture strategy, and other scaffold design parameters used in studies. Our wire inverse molding method had the lower limit for pore size, which was about 250 μm, but still was able to generate pPGD scaffold with a wide range of pore structural parameters that had the potential to optimize chondrocyte behaviors during neo-cartilage formation.

Articular cartilage transmits forces across joints and consequently the chondrocytes are exposed to a combination of compression, tension, and shear. These mechanical signals are critical regulators of cell behavior and function. It is well known that the magnitude and frequency of applied local strain cause distinct anabolic or catabolic outcomes in 2D chondrocyte loading experiments *in vitro*. Therefore, the magnitude and distribution of the local strains inside 3D scaffolds under loading is an important parameter to consider for scaffold design. Although the pPGD scaffolds provide a 3D environment for cell proliferation,

due to the large size of the pores created using the inverse molding method, these scaffolds still provide a 2D surface for cell attachment and mechanotransduction. According to the literature, loading between 3–10% cyclic tensile strain stimulates an anabolic response in monolayer culture. Below that range, the beneficial effect was negligible, and higher strains induce catabolic events to predominate. The effects of pore structural parameters on the strain field were analyzed using finite element analysis on the pPGD geometry. We found the maximum tensile strains that developed along pore surfaces inside of pPGD scaffolds were at levels shown to be beneficial to chondrocytes, except in the 1000 μm groups. The outcomes in the 1000 μm group may be caused in the geometry design step due to the large void space, leading to a large stress concentration. Coupling the pore structural parameters with local strain would provide a preliminary standard for matching up the local effects of these combined parameters on ECM production in future work.

4.6 Conclusion

The data acquired in this study showed that porous scaffolds that support chondrocyte anabolism could be generated from PGD using an inverse molding method. The pore size and porosity of pPGD were able to be adjusted by wire diameter or wire arrangement. FEA models of simulated pPGD structures showed that the majority of the internal pore surfaces in these scaffolds would experience strain fields that were proven to be beneficial to chondrocyte function under physiologic loads. Using this system in which the 3D pore structure (pore size and porosity) and compressive behavior can be tailored, this novel elastomer can be used as a platform to study how changes in length scale and organization of the engineered pore network affect matrix deposition *in vitro*, and how pore parameters interact with other scaffold parameters that also impact cell function, such as ligand presentation and stress/strain field

under loading, to change cell response to the microenvironment inside engineered scaffolds.

Chapter 5

Conclusions and Future Directions

Articular cartilage has a limited ability to self-repair, which often causes focal defects to progress into post-traumatic osteoarthritis (PTOA). Autologous chondrocyte implantation (ACI) is one of the most common approaches to treat cartilage defect but is limited by chondrocyte dedifferentiation during the expansion that results in loss of extracellular matrix so that cannot fully and durably restore cartilage function. Chondrocyte-based cartilage tissue engineering offers alternative approaches for cartilage repair to overcome the limitations of current clinical options and improve the outcome of cartilage regeneration, by engineering a construct involving cells, scaffolds, and biological or environmental factors. However, the translation of these newly engineered constructs to the clinic has been limited, and the main challenge in engineering cartilage construct is creating an appropriate culture environment to support chondrocyte redifferentiation and improve cartilage ECM production. There is an urgent need for a more complete understanding of the requirements of scaffold design parameters and the roles these parameters play in cartilage regeneration. The overall goal of this dissertation was to engineer a chondrocyte-based biomaterial platform made by poly (glycerol dodecanedioate) (PGD) that provides controls of key microenvironmental cues to support cartilage development and investigate the effects of scaffold design parameters on *in vitro* chondrocyte function. Three approaches were investigated to achieve this goal, including 1) generating surfaces coated with ligands on PGD to support chondrocyte growth and regulating its function by altering ligand type and/or density, 2) modifying PGD surface with

alkaline hydrolysis and regulating chondrocyte function by altering surface charge and/or roughness, 3) creating a 3D scaffold using PGD and regulating the cellular strain on pores by altering the pore structure.

The previous chapters described each above approach, presented key findings of the individual study, and discussed the relevance of their results in the field of cartilage tissue engineering. This chapter summarizes the conclusions of each study, provides a broad discussion that highlights the major impacts of each study in the field of tissue engineering, and introduced the future direction that could facilitate the application of PGD to the field.

5.1 Conclusion Summary

In Aim 1, this thesis evaluated the effects of surface modification of PGD on human articular chondrocyte function. To generate a biomaterial surface with high cell-affinity on PGD, I investigated two different strategies: 1) creating an ECM ligand-presenting environment and 2) modifying the charge density and roughness of surface by alkaline hydrolysis.

In Aim 1a, this thesis investigated effect of the component and density of cartilage ECM ligand on cell shape and cartilage matrix accumulation on PGD. Inducing cartilage ECM ligands on scaffolds can promote the formation of a cartilaginous matrix *in vitro*. I coated various amounts of collagen type I (Col I) or hyaluronic acid (HyA) individually or in combination on PGD films and cultured them with human articular chondrocyte (hAC) to evaluate chondrocyte responses to the ligand-presenting environment. There were notable effects of the ligand type on cell shape and ECM accumulation: HyA coated PGD induced a round cell shape, leading to higher ECM production, while Col I coated PGD induced polygonal cell shape. In addition to type of ligand coating, the ligand retention level, representing ligand density on PGD surface,

is another key parameter for chondrocyte function. Our results showed there were synergetic influences between ligand composition and ligand retention on ECM production. Coating with either HyA or Col I alone induced a dose-dependent response to the retention of both ligands on PGD. The combination of Col I and HyA, even with a higher HyA retention level, was not conducive to the higher ECM accumulation by HACs than HyA alone. Therefore, my results suggest there are combinatorial effects of ligand composition and density on human articular chondrocyte's function.

Due to hydrophobicity, the surface properties of PGD are not ideal for cell attachment and growth. Therefore, in Aim 1b, I determined how the level of surface charge and surface roughness influenced cell shape and cartilage matrix accumulation on PGD. This was accomplished by treating PGD with various levels of alkaline hydrolysis, via modifying alkaline concentration and treatment time, and culturing with hACs to evaluate chondrocyte responses to both surface charge level and surface micro-morphology. Our results indicated increasing the hydrolysis level led to higher surface charge density, however, this changed surface morphology by decreasing the surface roughness at first and then gradually increasing the roughness. A slightly rough surface with moderate surface charging resulted in a rounded cell shape and the highest ECM production, suggesting there were combinatorial influences of surface charge and morphology on cell functionality.

In Aim 2, I describe a novel approach to generating porous PGD scaffold with tailorable pore structure and investigate the effect of pore geometries on cellular-level strains that developed inside porous PGD scaffolds. Porous PGD scaffolds with tailorable pore size were successfully fabricated using an inverse molding approach. Our results demonstrated the maximum tensile strains that develop along > 60% pore surfaces inside porous PGD scaffolds, were at levels shown to be beneficial to chondrocyte anabolic activity. Porous PGD scaffolds with higher

porosity and smaller pore size tended to have a higher percentage of beneficial strain, suggesting that the pore structural parameters could be tuned to optimize cell-level strain profiles.

Overall, this dissertation presents a strategy for designing an ideal platform to support hAC redifferentiation using a novel bioelastomer, PGD. By stepwise parameterizing the bioelastomer platform for controlling important microenvironmental cues, this thesis successfully investigated the combinatorial influences of multiple scaffold design parameters on chondrocyte function.

5.2 Impact

Previous studies have established the importance of optimizing pore geometry and surface properties in engineered cartilage tissue constructs. Developing porous cartilage tissue scaffolds with tunable pore scale and organization will provide insights into how to intelligently design pore networks to optimize chondrocyte and neo-cartilage function. Pore geometry of the scaffold impacts the strain that cells may experience inside the pores, inspiring the approach to optimize cellular strain during 3D culture under loading to facilitate robust cartilaginous matrix production in a bioreactor system. Surface modification of PGD can balance out the less ideal properties of the PGD material itself. Notably, the crosstalk between the chondrocyte and the ligand-coated surface of the scaffold remains for further exploration. Our results suggested there were combinatorial effects of ligand density, type, and coating approach on chondrocyte function, suggesting that the crosstalk between cell and ligand could be regulated by both the number and the type of ligand that the cell is sensing. Our PGD 2D model has the ability to investigate the optimal combination of ligand coating and cell seeding density in monolayer

culture and has the potential to prevent chondrocyte dedifferentiation during monolayer expansion. Similarly, there were combinatorial effects of surface charge and roughness on chondrocyte function, suggesting that the chondrocyte function could be optimized by regulating these parameters. Creation of free carboxyl groups and hydroxyl groups on the surface of PGD will provide the opportunity for further surface modification, which may broaden the application of this novel biomaterial in the field of tissue engineering. With further adjustments in those parameters, an ideal scaffold for cartilage tissue engineering to support chondrocyte redifferentiation and cartilage regeneration may be achieved.

According to the findings in both Aim 1 and Aim 2, the PGD scaffold with well-defined pore and surface parameters has the potential to serve as cell-based regenerative therapy to treat articular cartilage injury and prevent PTOA. This thesis provides a reasonable approach to optimize scaffold design for cartilage engineering and investigate the mechanistic regulation of scaffold parameters on chondrocyte function for tissue engineering purposes, which will be a significant push toward the clinical application of chondrocytes-based cartilage defect repair using PGD or other elastomers with similar polyester properties and nonlinear elasticity.

5.3 Future Directions

5.3.1 Optimizing 3D Scaffold Design for PGD

The immediate future work is to understand the effects of the combination of scaffold design parameters on ECM production in 3D culture. This dissertation developed attractive strategies for optimizing scaffold design in (1) 2D setting: surface parameters, (2) 3D setting: pore structure and corresponding local strain field. However, these study designs were not combined to demonstrate the combinatorial effect of PGD surface properties and pore structure on

chondrocyte behavior. The optimal 3D scaffold design requires knowledge of the effects of surface modification on guiding cell behavior in a 3D setting. Our understanding of the roles that surface properties plays in regulating chondrocyte behavior in a 2D setting, gathered from Aim 1, will facilitate the pre-design of the parameters in the 3D scaffold. However, chondrocyte behavior may alter from what was found in 2D culture when cultured in 3D environments. Moreover, although this thesis showed that the ECM outcomes on surface-modified PGD have been successful in mimicking the biochemical appearance of hyaline cartilage, it is usually mechanically inferior to the natural tissue and requires a long-term culture period to develop the load-bearing properties. Therefore, to find an optimal combination of scaffold parameters in porous PGD scaffolds, we need to co-culture chondrocytes with porous PGD scaffolds with various design parameters to test the combinatorial effects of ligand/surface functional groups and pore geometry on chondrocyte function in the 3D environment in long-term culture.

There are some approaches that could potentially improve chondrocyte biosynthesis response in 3D culture in addition to the surface modification approaches in this thesis. One of the ways to further improved PGD's surface properties is to develop a biomimetic PGD surface to promote cartilage tissue engineering outcomes. Studies have shown that immobilized ligands or biomimetic peptides successfully improve cell growth and function [99, 100]. Functionalizing the ECM ligand, e.g., collagen, on the scaffold surface improves the ability to control the ligand density that cell sense inside the pores and enhances the stability of cell-matrix connections. In this thesis, functional groups such as carboxyl group and hydroxyl group were generated on the surface of PGD via hydrolysis treatment, which broaden the opportunity for further surface modification to improve chondrocyte attachment and function, for example, creating biomimetic scaffold by covalently binding peptides, such as transforming growth factor-β mimetic peptides, RGD, and CD-44 affinity peptides. Developing versatile biomimetic PGD surfaces via covalently binding ligands or functional peptides can enhance not only

cartilage-specific matrix production but also the tissue regenerative capability of PGD scaffold in other tissues, which greatly broadens the application of this novel bioelastomer.

5.3.2 Promote Cartilage Matrix Quality with Mechanical Stimulus

One of the prevailing approaches for improving long-term outcomes of the implantation of tissue-engineered construct *in vivo* is functional tissue engineering (FTE). This approach is to first cultivate constructs *in vitro* to allow the elaboration of extracellular matrix using physiologic loading bioreactor systems before implantation, and finally to create functional load-bearing properties of articular cartilage [101, 102]. Studies have shown that the anabolic activity of chondrocytes is strongly dependent on the magnitude and frequency of the applied strain [72, 103]. In this thesis, the cellular strain developed inside the pores of PGD scaffold was highly coupled with pore size and porosity, suggesting an approach to adjust the cellular strain that cells could experience inside the scaffold during bioreactor culture. However, the finite element models (FEM) used in this thesis did not consider the time component upon cartilage development. Both cell-cell interaction and cell-matrix interaction can change in a 3D environment during *in vitro* culture so the current model cannot satisfy the final goal of predicting the cellular strain in 3D culture during cyclic loading. Therefore, the next step is to develop a finite element model with a time-dependent component mimicking the mechanical properties of neo-cartilage matrix, and then assess the contribution of cellular strain to cartilage regenerative outcomes in 3D culture under cyclic load. To be specific, we can spatiotemporally investigate the quality of neo-ECM formed inside porous PGD scaffold coupling with the results of predicted strain field in scaffolds using nano-CT with contract agent and FEM, to see if there is a co-locating relationship between healthy neo-ECM and certain cellular strain level. The possible outcomes of ECM production of the construct will be predictable via

computational modeling procedures, which will greatly improve the efficiency of scaffold design for enhancing cartilage function. By optimizing the ECM quality after *in vitro* bioreactor culture, this biomaterial system will be reliable to apply in future *in vivo* studies.

5.3.3 Promote Cartilage Tissue Mechanics by Zonal Constructs

The initial goal for cartilage tissue engineering was to make a homogeneous tissue *in vitro* that mimicked the overall bulk properties of native articular cartilage. The pore arrangement of 3D PGD scaffold in this dissertation is designed to be homogeneous and isotropic. However, natural articular cartilage has a heterogeneous and anisotropic microstructure that is organized into distinct regions (**Figure 5.1 a**). The morphology and function of the chondrocyte and the surrounding composition of the ECM have depth-dependent differences across the superficial zone to the deep zone in articular cartilage [104, 105]. This structural integrity of articular cartilage is necessary to maintain physical and mechanical competence, reactivity to load transmission, and a low-friction surface [106-108]. Therefore, the goal for treating cartilage full-thickness defect is to build a 3D construct mimicking the heterogeneity of native cartilage or including zonal structure, thus enhancing the load-bearing properties and wear resistance of the implants. Studies have used salt-particle leaching and electrospinning approaches to create a bilayer construct that mimics the functional interfaces of cartilage tissue as well as supporting *in vitro* cartilage formation [109]. Zonal constructs also can facilitate neo-cartilage–cartilage integration by matching the mechanical properties to the surrounding tissues to reduce strain discontinuities at the interface [107]. However, the interfaces between the layers of the zonal construct may lead to crack and stress concentration to chondrocytes [110] in the complex biomechanical environment during long-term *in vivo* study. In this thesis, we successfully created a well-defined porous structure with tailorable pore size, porosity, pore spacing, pore

density, and pore orientation in PGD scaffold using a wire inverse modeling method, establishing the fundamental techniques to create zonal cartilage-mimicking structures without having zonal interfaces using PGD. Salt-particle leaching is also a way to control the pore geometry in PGD scaffold, since it was proved to fit the purpose of creating a structure that mimics the middle and deep zone of cartilage [109]. Our preliminary data of microCT images of porous PGD scaffolds created by salt-particle leaching showed a successful control of interconnected pore structures with varying pore diameters (**Figure 5.1 b**). By optimizing the zonal pore structure and neo-cartilage ECM quality, this platform system will gain compelling potential for application to pre-clinical studies.

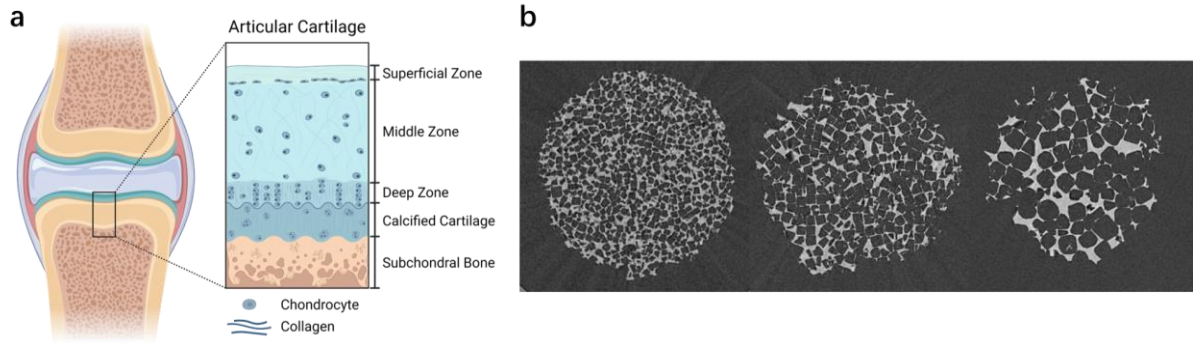

Figure 5.1 Rationales of designing zonal scaffolds for cartilage tissue engineering. (a) Schematic depiction of the zonal structure of articular cartilage at the joint surface. (b) The μCT images of porous PGD scaffolds (cross-section) with varying pore diameters created by salt-particle leaching.

5.3.4 Evaluate Regenerative Effects *in vivo*

The next steps require a proper *in vivo* study to accurately recapitulate a cartilage defect using an optimized 3D PGD scaffold to truly assess the regenerative potential of the scaffold generated in this dissertation. This involves the validation of the finite element model and optimized design parameters mentioned in previous sections with a proper pre-clinical model. Animal models are widely used to evaluate novel approaches for regenerative cartilage defect treatment. However, it is a challenge to find the perfect animal model that precisely mimics the human [111]. Studies suggest that the small animal model like rabbit does fully recapitulate

critical-sized cartilage defect, however, there are still differences in the scale of human patients (~ 550 mm^3 defects in volume) versus small animal models [111]. Though the relatively low cost and simple husbandry make smaller animal models ideal, large animal models such as the goat or the horse may more closely resemble the human. In this thesis, our ultimate goal is to design an optimal PGD scaffold that can fully restore cartilage function and serve as long-term biological treatment in the defect site of the human joints. Therefore, it is necessary to choose a small animal model for initial lines of investigation, while the final preclinical evaluation of this reconstruction technique may require confirmation in a large animal model. After confirming the regenerative effects of our PGD platform via *in vivo* studies, we will establish a feasible deign-test strategy that could help streamline the creation of new thermoset polymeric scaffolds for tissue engineering purposes, by step-wisely optimizing scaffold design parameters, to ultimately support *in vitro* tissue regeneration and restore tissue function in long-term pre-clinical studies.

5.3.4 Potential Bioelastomers for Tissue Regenerative Purpose

Aliphatic polyol polyesters, such as poly(glycerol sebacate) (PGS) [63, 112] and poly(glycerol dodecanedioate) (PGD) [47, 113], are an emerging and promising class of thermosetting elastomers that were proved to have potential in applying in soft tissue engineering. This class of polyesters was synthesized via straightforward polycondensation of nontoxic metabolic compounds in the human body, glycerol, and even-numbered dicarboxylic acids (sebacic acid and dodecanedioic acid, respectively). Poly (glycerol dodecanedioate) (PGD) used in this thesis is a novel biodegradable polyester elastomer formed by polycondensation of glycerol and dodecanedioic acid with a molar ratio of 1:1. Because of their biocompatibility, biodegradability, non-toxic biodegradation products, nonlinear elastomeric mechanical

properties, shape-memory behavior, and mechanical stability, PGS and PGD have been exploited as scaffolding materials in various soft tissue engineering applications [114-116]. They can tolerate being sterilized by exposure to high temperatures, ethylene oxide vapor, and gamma radiation due to their high curing temperatures. Therefore, aliphatic polyol polyesters have been proposed as a biodegradable candidate for tissue engineering scaffolds and medical devices.

Because the soft tissues, such as nerves, blood vessels, cardiac muscles, and cartilage in the body showed different functions and regeneration rates, the polyester elastomers with tunable material properties and degradation rates are highly desirable for regenerative purposes. The chemical structures, mechanical properties, and physicochemical properties of the polyester elastomers can be tailored to match the specific tissue requirements by altering processing parameters such as reaction atmosphere, the molar ratio of the reactants, the reaction temperature, and/or time of the pre-polymerization and/or thermal-curing stages [47, 74, 112, 117-119]. Therefore, based on our experiences in studying PGD, we can formulate a group of elastomers with various molar ratios of dicarboxylic acids and glycerol, curing conditions, and carbon chain length of the dicarboxylic acid monomer, to 1) provide a better understanding of the relationships between chemical structure and properties of an elastomer, 2) screen out the feasible elastomer formula for particular soft tissue engineering applications.

Bibliography

1. Thomas, A.C., et al., *Epidemiology of posttraumatic osteoarthritis.* Journal of athletic training, 2017. **52**(6): p. 491-496.
2. Safiri, S., et al., *Global, regional and national burden of osteoarthritis 1990-2017: a systematic analysis of the Global Burden of Disease Study 2017.* Annals of the rheumatic diseases, 2020. **79**(6): p. 819-828.
3. Davies, R.L. and N.J. Kuiper, *Regenerative medicine: a review of the evolution of autologous chondrocyte implantation (ACI) therapy.* Bioengineering, 2019. **6**(1): p. 22.
4. Zhang, L., J. Hu, and K.A. Athanasiou, *The role of tissue engineering in articular cartilage repair and regeneration.* Critical Reviews™ in Biomedical Engineering, 2009. **37**(1-2).
5. Hollister, S.J., *Scaffold design and manufacturing: from concept to clinic.* Advanced materials, 2009. **21**(32-33): p. 3330-3342.
6. Allemann, F., et al., *Effects of hyaluronan on engineered articular cartilage extracellular matrix gene expression in 3-dimensional collagen scaffolds.* Journal of Biomedical Materials Research: An Official Journal of The Society for Biomaterials, The Japanese Society for Biomaterials, and The Australian Society for Biomaterials and the Korean Society for Biomaterials, 2001. **55**(1): p. 13-19.
7. Kim, T.G., H. Shin, and D.W. Lim, *Biomimetic scaffolds for tissue engineering.* Advanced Functional Materials, 2012. **22**(12): p. 2446-2468.
8. Chen, C.-H., et al., *Surface modification of polycaprolactone scaffolds fabricated via selective laser sintering for cartilage tissue engineering.* Materials Science and Engineering: C, 2014. **40**: p. 389-397.
9. Boyan, B.D., et al., *Role of material surfaces in regulating bone and cartilage cell response.* Biomaterials, 1996. **17**(2): p. 137-146.
10. Studer, D., et al., *Molecular and biophysical mechanisms regulating hypertrophic differentiation in chondrocytes and mesenchymal stem cells.* Eur Cell Mater, 2012. **24**(24): p. 118-135.
11. Boland, E.D., et al., *Utilizing acid pretreatment and electrospinning to improve biocompatibility of poly (glycolic acid) for tissue engineering.* Journal of Biomedical Materials Research Part B: Applied Biomaterials: An Official Journal of The Society for Biomaterials, The Japanese Society for Biomaterials, and The Australian Society for Biomaterials and the Korean Society for Biomaterials, 2004. **71**(1): p. 144-152.
12. Rampichová, M., et al., *Non-woven PGA/PVA fibrous mesh as an appropriate scaffold for chondrocyte proliferation.* Physiological Research, 2010.
13. Janvikul, W., et al., *Effects of surface topography, hydrophilicity and chemistry of surface-treated PCL scaffolds on chondrocyte infiltration and ECM production.* Procedia Engineering, 2013. **59**: p. 158-165.
14. Lee, J.-W. and J.A. Gardella, *In vitro hydrolytic surface degradation of poly (glycolic acid): Role of the surface segregated amorphous region in the induction period of bulk erosion.* Macromolecules, 2001. **34**(12): p. 3928-3937.
15. Cheng, A., et al., *Advances in porous scaffold design for bone and cartilage tissue*

engineering and regeneration. Tissue Engineering Part B: Reviews, 2019. **25**(1): p. 14-29.
16. Gao, Y., et al., *The ECM-cell interaction of cartilage extracellular matrix on chondrocytes.* BioMed research international, 2014. **2014**.
17. Maldonado, M. and J. Nam, *The role of changes in extracellular matrix of cartilage in the presence of inflammation on the pathology of osteoarthritis.* BioMed research international, 2013. **2013**.
18. Akkiraju, H. and A. Nohe, *Role of chondrocytes in cartilage formation, progression of osteoarthritis and cartilage regeneration.* Journal of developmental biology, 2015. **3**(4): p. 177-192.
19. Kreuz, P., et al., *Results after microfracture of full-thickness chondral defects in different compartments in the knee.* Osteoarthritis and cartilage, 2006. **14**(11): p. 1119-1125.
20. Solheim, E., et al., *Results at 10–14 years after microfracture treatment of articular cartilage defects in the knee.* Knee Surgery, Sports Traumatology, Arthroscopy, 2016. **24**(5): p. 1587-1593.
21. Miyata, S., et al., *Influence of structure and composition on dynamic viscoelastic property of cartilaginous tissue: criteria for classification between hyaline cartilage and fibrocartilage based on mechanical function.* JSME International Journal Series C Mechanical Systems, Machine Elements and Manufacturing, 2005. **48**(4): p. 547-554.
22. Williams, S.K., et al., *Prolonged storage effects on the articular cartilage of fresh human osteochondral allografts.* JBJS, 2003. **85**(11): p. 2111-2120.
23. Camp, C.L., M.J. Stuart, and A.J. Krych, *Current concepts of articular cartilage restoration techniques in the knee.* Sports health, 2014. **6**(3): p. 265-273.
24. Martinčič, D., J. Mekač, and M. Drobnič, *Survival rates of various autologous chondrocyte grafts and concomitant procedures. A prospective single-center study over 18 years.* Cell Transplantation, 2019. **28**(11): p. 1439-1444.
25. Bobacz, K., et al., *Chondrocyte number and proteoglycan synthesis in the aging and osteoarthritic human articular cartilage.* Annals of the rheumatic diseases, 2004. **63**(12): p. 1618-1622.
26. Kreuz, P., et al., *Classification of graft hypertrophy after autologous chondrocyte implantation of full-thickness chondral defects in the knee.* Osteoarthritis and cartilage, 2007. **15**(12): p. 1339-1347.
27. Albrecht, C., et al., *Gene expression and cell differentiation in matrix-associated chondrocyte transplantation grafts: a comparative study.* Osteoarthritis and cartilage, 2011. **19**(10): p. 1219-1227.
28. Stewart, M.C., et al., *Phenotypic stability of articular chondrocytes in vitro: the effects of culture models, bone morphogenetic protein 2, and serum supplementation.* Journal of bone and mineral research, 2000. **15**(1): p. 166-174.
29. Aulthouse, A.L., et al., *Expression of the human chondrocyte phenotype in vitro.* In vitro cellular & developmental biology, 1989. **25**(7): p. 659-668.
30. Hubka, K.M., et al., *Enhancing chondrogenic phenotype for cartilage tissue engineering: monoculture and coculture of articular chondrocytes and mesenchymal stem cells.* Tissue Engineering Part B: Reviews, 2014. **20**(6): p. 641-654.
31. Glowacki, J., E. Trepman, and J. Folkman, *Cell shape and phenotypic expression in chondrocytes.* Proceedings of the Society for Experimental Biology and Medicine, 1983. **172**(1): p. 93-98.
32. Caliari, S.R. and J.A. Burdick, *A practical guide to hydrogels for cell culture.* Nature methods, 2016. **13**(5): p. 405-414.
33. Chung, C. and J.A. Burdick, *Engineering cartilage tissue.* Advanced drug delivery

reviews, 2008. **60**(2): p. 243-262.
34. Endres, M., et al., *An ovine in vitro model for chondrocyte-based scaffold-assisted cartilage grafts.* Journal of orthopaedic surgery and research, 2012. **7**(1): p. 1-14.
35. Mhanna, R., et al., *Chondrocyte culture in three dimensional alginate sulfate hydrogels promotes proliferation while maintaining expression of chondrogenic markers.* Tissue Engineering Part A, 2014. **20**(9-10): p. 1454-1464.
36. Mobasheri, A., et al., *Chondrocyte and mesenchymal stem cell-based therapies for cartilage repair in osteoarthritis and related orthopaedic conditions.* Maturitas, 2014. **78**(3): p. 188-198.
37. Temenoff, J.S. and A.G. Mikos, *Tissue engineering for regeneration of articular cartilage.* Biomaterials, 2000. **21**(5): p. 431-440.
38. Schulze-Tanzil, G., *Activation and dedifferentiation of chondrocytes: implications in cartilage injury and repair.* Annals of Anatomy-Anatomischer Anzeiger, 2009. **191**(4): p. 325-338.
39. Adachi, T., et al., *Framework for optimal design of porous scaffold microstructure by computational simulation of bone regeneration.* Biomaterials, 2006. **27**(21): p. 3964-3972.
40. Elhadad, A.A., et al., *A multidisciplinary perspective on the latest trends in artificial cartilage fabrication to mimic real tissue.* Applied Materials Today, 2022. **29**: p. 101603.
41. Girão, A.F., et al., *Mimicking nature: fabrication of 3D anisotropic electrospun polycaprolactone scaffolds for cartilage tissue engineering applications.* Composites Part B: Engineering, 2018. **154**: p. 99-107.
42. Song, R., et al., *Current development of biodegradable polymeric materials for biomedical applications.* Drug design, development and therapy, 2018. **12**: p. 3117.
43. Ramaraju, H., et al., *Modulating nonlinear elastic behavior of biodegradable shape memory elastomer and small intestinal submucosa (SIS) composites for soft tissue repair.* Journal of the Mechanical Behavior of Biomedical Materials, 2020. **110**: p. 103965.
44. Kang, Y., et al., *A new biodegradable polyester elastomer for cartilage tissue engineering.* Journal of Biomedical Materials Research Part A: An Official Journal of The Society for Biomaterials, The Japanese Society for Biomaterials, and The Australian Society for Biomaterials and the Korean Society for Biomaterials, 2006. **77**(2): p. 331-339.
45. Rai, R., et al., *Synthesis, properties and biomedical applications of poly (glycerol sebacate)(PGS): A review.* Progress in polymer science, 2012. **37**(8): p. 1051-1078.
46. Migneco, F., et al., *Poly (glycerol-dodecanoate), a biodegradable polyester for medical devices and tissue engineering scaffolds.* Biomaterials, 2009. **30**(33): p. 6479-6484.
47. Solorio, L.D., M.L. Bocks, and S.J. Hollister, *Tailoring the physicochemical and shape memory properties of the biodegradable polymer poly (glycerol dodecanoate) via curing conditions.* Journal of Biomedical Materials Research Part A, 2017. **105**(6): p. 1618-1623.
48. Jeong, C.G. and S.J. Hollister, *A comparison of the influence of material on in vitro cartilage tissue engineering with PCL, PGS, and POC 3D scaffold architecture seeded with chondrocytes.* Biomaterials, 2010. **31**(15): p. 4304-4312.
49. Yamane, S., et al., *Effect of pore size on in vitro cartilage formation using chitosan-based hyaluronic acid hybrid polymer fibers.* Journal of Biomedical Materials Research Part A, 2007. **81**(3): p. 586-593.
50. Stenhamre, H., et al., *Influence of pore size on the redifferentiation potential of human articular chondrocytes in poly (urethane urea) scaffolds.* Journal of tissue engineering and regenerative medicine, 2011. **5**(7): p. 578-588.

51. Kino-Oka, M., et al., *Subculture of chondrocytes on a collagen type I-coated substrate with suppressed cellular dedifferentiation.* Tissue engineering, 2005. **11**(3-4): p. 597-608.
52. Brodkin, K., A. Garcıa, and M. Levenston, *Chondrocyte phenotypes on different extracellular matrix monolayers.* Biomaterials, 2004. **25**(28): p. 5929-5938.
53. Grigolo, B., et al., *Down regulation of degenerative cartilage molecules in chondrocytes grown on a hyaluronan-based scaffold.* Biomaterials, 2005. **26**(28): p. 5668-5676.
54. Liao, E., et al., *Tissue-engineered cartilage constructs using composite hyaluronic acid/collagen I hydrogels and designed poly (propylene fumarate) scaffolds.* Tissue engineering, 2007. **13**(3): p. 537-550.
55. Saini, S. and T.M. Wick, *Concentric cylinder bioreactor for production of tissue engineered cartilage: effect of seeding density and hydrodynamic loading on construct development.* Biotechnology progress, 2003. **19**(2): p. 510-521.
56. Watt, F.M., *Effect of seeding density on stability of the differentiated phenotype of pig articular chondrocytes in culture.* Journal of cell science, 1988. **89**(3): p. 373-378.
57. Cao, C., et al., *Effects of cell phenotype and seeding density on the chondrogenic capacity of human osteoarthritic chondrocytes in type I collagen scaffolds.* Journal of Orthopaedic Surgery and Research, 2020. **15**: p. 1-11.
58. Gaudet, C., et al., *Influence of type I collagen surface density on fibroblast spreading, motility, and contractility.* Biophysical journal, 2003. **85**(5): p. 3329-3335.
59. Von Der Mark, K., et al., *Relationship between cell shape and type of collagen synthesised as chondrocytes lose their cartilage phenotype in culture.* Nature, 1977. **267**(5611): p. 531-532.
60. Benya, P.D., S.R. Padilla, and M.E. Nimni, *Independent regulation of collagen types by chondrocytes during the loss of differentiated function in culture.* Cell, 1978. **15**(4): p. 1313-1321.
61. Chahine, N.O., et al., *Nanocomposite scaffold for chondrocyte growth and cartilage tissue engineering: effects of carbon nanotube surface functionalization.* Tissue Engineering Part A, 2014. **20**(17-18): p. 2305-2315.
62. Chen, J.-P. and C.-H. Su, *Surface modification of electrospun PLLA nanofibers by plasma treatment and cationized gelatin immobilization for cartilage tissue engineering.* Acta biomaterialia, 2011. **7**(1): p. 234-243.
63. Theerathanagorn, T., et al., *In vitro human chondrocyte culture on plasma-treated poly (glycerol sebacate) scaffolds.* Journal of Biomaterials Science, Polymer Edition, 2015. **26**(18): p. 1386-1401.
64. Cui, Y.L., et al., *Biomimetic surface modification of poly (L-lactic acid) with chitosan and its effects on articular chondrocytes in vitro.* Biomaterials, 2003. **24**(21): p. 3859-3868.
65. Ma, Z., et al., *Chondrocyte behaviors on poly-L-lactic acid (PLLA) membranes containing hydroxyl, amide or carboxyl groups.* Biomaterials, 2003. **24**(21): p. 3725-3730.
66. Reilly, G.C. and A.J. Engler, *Intrinsic extracellular matrix properties regulate stem cell differentiation.* Journal of biomechanics, 2010. **43**(1): p. 55-62.
67. Genes, N.G., et al., *Effect of substrate mechanics on chondrocyte adhesion to modified alginate surfaces.* Archives of biochemistry and biophysics, 2004. **422**(2): p. 161-167.
68. Allen, J.L., M.E. Cooke, and T. Alliston, *ECM stiffness primes the TGFβ pathway to promote chondrocyte differentiation.* Molecular biology of the cell, 2012. **23**(18): p. 3731-3742.
69. Cai, L., et al., *Biomaterial stiffness guides crosstalk between chondrocytes:*

Implications for a novel cellular response in cartilage tissue engineering. ACS Biomaterials Science & Engineering, 2020.
70. Mauck, R.L., et al., *Synergistic action of growth factors and dynamic loading for articular cartilage tissue engineering.* Tissue engineering, 2003. **9**(4): p. 597-611.
71. Szafranski, J.D., et al., *Chondrocyte mechanotransduction: effects of compression on deformation of intracellular organelles and relevance to cellular biosynthesis.* Osteoarthritis and cartilage, 2004. **12**(12): p. 937-946.
72. Bleuel, J., et al., *Effects of cyclic tensile strain on chondrocyte metabolism: a systematic review.* PLoS One, 2015. **10**(3): p. e0119816.
73. Zopf, D.A., et al., *Biomechanical evaluation of human and porcine auricular cartilage.* The Laryngoscope, 2015. **125**(8): p. E262-E268.
74. Ramaraju, H., et al., *Degradation properties of a biodegradable shape memory elastomer, poly (glycerol dodecanoate), for soft tissue repair.* Plos one, 2020. **15**(2): p. e0229112.
75. Rutgers, M., et al., *Effect of collagen type I or type II on chondrogenesis by cultured human articular chondrocytes.* Tissue Engineering Part A, 2013. **19**(1-2): p. 59-65.
76. Curran, J., R. Chen, and J. Hunt, *Controlling the phenotype and function of mesenchymal stem cells in vitro by adhesion to silane-modified clean glass surfaces.* Biomaterials, 2005. **26**(34): p. 7057-7067.
77. Gao, J., L. Niklason, and R. Langer, *Surface hydrolysis of poly (glycolic acid) meshes increases the seeding density of vascular smooth muscle cells.* Journal of Biomedical Materials Research: An Official Journal of The Society for Biomaterials, The Japanese Society for Biomaterials, and the Australian Society for Biomaterials, 1998. **42**(3): p. 417-424.
78. Kosorn, W., et al., *Chondrogenic phenotype in responses to poly (ε-caprolactone) scaffolds catalyzed by bioenzymes: effects of surface topography and chemistry.* Journal of Materials Science: Materials in Medicine, 2019. **30**(12): p. 1-15.
79. Koshimizu, T., et al., *Vinculin functions as regulator of chondrogenesis.* Journal of Biological Chemistry, 2012. **287**(19): p. 15760-15775.
80. Kurtis, M.S., et al., *Integrin-mediated adhesion of human articular chondrocytes to cartilage.* Arthritis & Rheumatism, 2003. **48**(1): p. 110-118.
81. Loeser, R.F., *Integrins and chondrocyte–matrix interactions in articular cartilage.* Matrix Biology, 2014. **39**: p. 11-16.
82. Yoo, H.S., et al., *Hyaluronic acid modified biodegradable scaffolds for cartilage tissue engineering.* Biomaterials, 2005. **26**(14): p. 1925-1933.
83. Mankin, H.J., *The response of articular cartilage to mechanical injury.* JBJS, 1982. **64**(3): p. 460-466.
84. Phull, A.-R., et al., *Applications of chondrocyte-based cartilage engineering: an overview.* BioMed research international, 2016. **2016**.
85. Wang, S., et al., *Polymeric biomaterials for tissue engineering applications*. 2010, Hindawi.
86. Nikolova, M.P. and M.S. Chavali, *Recent advances in biomaterials for 3D scaffolds: A review.* Bioactive materials, 2019. **4**: p. 271-292.
87. Jeong, C.G. and S.J. Hollister, *Mechanical and biochemical assessments of three-dimensional poly (1, 8-octanediol-co-citrate) scaffold pore shape and permeability effects on in vitro chondrogenesis using primary chondrocytes.* Tissue Engineering Part A, 2010. **16**(12): p. 3759-3768.
88. Jeong, C.G., H. Zhang, and S.J. Hollister, *Three-dimensional poly (1, 8-octanediol–co-citrate) scaffold pore shape and permeability effects on sub-cutaneous in vivo chondrogenesis using primary chondrocytes.* Acta biomaterialia, 2011. **7**(2): p. 505-514.

89. Selig, M., et al., *Mechanotransduction and stiffness-sensing: mechanisms and opportunities to control multiple molecular aspects of cell phenotype as a design cornerstone of cell-instructive biomaterials for articular cartilage repair.* International journal of molecular sciences, 2020. **21**(15): p. 5399.
90. Halonen, K., et al., *Deformation of articular cartilage during static loading of a knee joint–experimental and finite element analysis.* Journal of biomechanics, 2014. **47**(10): p. 2467-2474.
91. Haider, A., et al., *Advances in the scaffolds fabrication techniques using biocompatible polymers and their biomedical application: A technical and statistical review.* Journal of saudi chemical society, 2020. **24**(2): p. 186-215.
92. Annabi, N., et al., *Controlling the porosity and microarchitecture of hydrogels for tissue engineering.* Tissue Engineering Part B: Reviews, 2010. **16**(4): p. 371-383.
93. Dhandayuthapani, B., et al., *Polymeric scaffolds in tissue engineering application: a review.* International journal of polymer science, 2011. **2011**.
94. Yu, G. and Y. Fan, *Preparation of poly (D, L-lactic acid) scaffolds using alginate particles.* Journal of Biomaterials Science, Polymer Edition, 2008. **19**(1): p. 87-98.
95. Liao, C.J., et al., *Fabrication of porous biodegradable polymer scaffolds using a solvent merging/particulate leaching method.* Journal of Biomedical Materials Research: An Official Journal of The Society for Biomaterials, The Japanese Society for Biomaterials, and The Australian Society for Biomaterials and the Korean Society for Biomaterials, 2002. **59**(4): p. 676-681.
96. Park, H., et al., *The significance of pore microarchitecture in a multi-layered elastomeric scaffold for contractile cardiac muscle constructs.* Biomaterials, 2011. **32**(7): p. 1856-1864.
97. Samourides, A., et al., *Fabrication of Hierarchical Multilayer Poly (Glycerol Sebacate urethane) Scaffolds Based on Ice-Templating.* Applied Sciences, 2021. **11**(11): p. 5004.
98. Ribeiro, V.P., et al., *Combinatory approach for developing silk fibroin scaffolds for cartilage regeneration.* Acta biomaterialia, 2018. **72**: p. 167-181.
99. Rai, R., et al., *Biomimetic poly (glycerol sebacate)(PGS) membranes for cardiac patch application.* Materials Science and Engineering: C, 2013. **33**(7): p. 3677-3687.
100. Lee, K.-B., et al., *Surface modification of poly (glycolic acid)(PGA) for biomedical applications.* Journal of pharmaceutical sciences, 2003. **92**(5): p. 933-937.
101. Guilak, F., D.L. Butler, and S.A. Goldstein, *Functional tissue engineering: the role of biomechanics in articular cartilage repair.* Clinical Orthopaedics and Related Research®, 2001. **391**: p. S295-S305.
102. Mauck, R.L., et al., *Functional tissue engineering of articular cartilage through dynamic loading of chondrocyte-seeded agarose gels.* Journal of biomechanical engineering, 2000. **122**(3): p. 252-260.
103. Sah, R.L.Y., et al., *Biosynthetic response of cartilage explants to dynamic compression.* Journal of orthopaedic research, 1989. **7**(5): p. 619-636.
104. Hunziker, E., T. Quinn, and H.-J. Häuselmann, *Quantitative structural organization of normal adult human articular cartilage.* Osteoarthritis and Cartilage, 2002. **10**(7): p. 564-572.
105. Poole, A.R., et al., *Composition and structure of articular cartilage: a template for tissue repair.* Clinical Orthopaedics and Related Research®, 2001. **391**: p. S26-S33.
106. Klein, T.J., et al., *Depth-dependent biomechanical and biochemical properties of fetal, newborn, and tissue-engineered articular cartilage.* Journal of biomechanics, 2007. **40**(1): p. 182-190.
107. Klein, T.J., et al., *Tissue engineering of articular cartilage with biomimetic zones.* Tissue Engineering Part B: Reviews, 2009. **15**(2): p. 143-157.

108. Franz, T., et al., *In situ compressive stiffness, biochemical composition, and structural integrity of articular cartilage of the human knee joint.* Osteoarthritis and Cartilage, 2001. **9**(6): p. 582-592.
109. Steele, J., et al., *Combinatorial scaffold morphologies for zonal articular cartilage engineering.* Acta biomaterialia, 2014. **10**(5): p. 2065-2075.
110. Liu, H.-Y., et al., *Study of the mechanical environment of chondrocytes in articular cartilage defects repaired area under cyclic compressive loading.* Journal of healthcare engineering, 2017. **2017**.
111. Ahern, B., et al., *Preclinical animal models in single site cartilage defect testing: a systematic review.* Osteoarthritis and cartilage, 2009. **17**(6): p. 705-713.
112. Kemppainen, J.M. and S.J. Hollister, *Tailoring the mechanical properties of 3D-designed poly (glycerol sebacate) scaffolds for cartilage applications.* Journal of Biomedical Materials Research Part A: An Official Journal of The Society for Biomaterials, The Japanese Society for Biomaterials, and The Australian Society for Biomaterials and the Korean Society for Biomaterials, 2010. **94**(1): p. 9-18.
113. Dai, X., K. Kathiria, and Y.-C. Huang, *Electrospun fiber scaffolds of poly (glycerol-dodecanedioate) and its gelatin blended polymers for soft tissue engineering.* Biofabrication, 2014. **6**(3): p. 035005.
114. Ramaraju, H., et al., *Designing biodegradable shape memory polymers for tissue repair.* Advanced Functional Materials, 2020. **30**(44): p. 2002014.
115. Pomerantseva, I., et al., *Degradation behavior of poly (glycerol sebacate).* Journal of Biomedical Materials Research Part A: An Official Journal of The Society for Biomaterials, The Japanese Society for Biomaterials, and The Australian Society for Biomaterials and the Korean Society for Biomaterials, 2009. **91**(4): p. 1038-1047.
116. Wang, Y., et al., *Optimized synthesis of biodegradable elastomer pegylated poly (glycerol sebacate) and their biomedical application.* Polymers, 2019. **11**(6): p. 965.
117. Frydrych, M. and B. Chen, *Large three-dimensional poly (glycerol sebacate)-based scaffolds–a freeze-drying preparation approach.* Journal of Materials Chemistry B, 2013. **1**(48): p. 6650-6661.
118. Chen, Q.-Z., et al., *Characterisation of a soft elastomer poly (glycerol sebacate) designed to match the mechanical properties of myocardial tissue.* Biomaterials, 2008. **29**(1): p. 47-57.
119. Liu, Y., et al., *Biomimetic poly (glycerol sebacate)/polycaprolactone blend scaffolds for cartilage tissue engineering.* Journal of Materials Science: Materials in Medicine, 2019. **30**(5): p. 1-11.